THE UNIVERSITY OF MICHIGAN

INDUSTRY PROGRAM OF THE COLLEGE OF ENGINEERING

LIQUID-LIQUID EQUILIBRIA AND THERMODYNAMIC DATA FOR THE Fe-C-Si-Mg SYSTEM

Paul K. Trojan

June, 1961

IP-518

PREFACE

I wish to express my appreciation to all those who have aided in this investigation and particularly to the following:

Professor Richard A. Flinn, Chairman of the Doctoral Committee for his encouragement, suggestions, critical analyses, and necessary patience during the long course of this investigation.

Professors L. O. Case and D. V. Ragone, members of the Doctoral Committee for their friendly advice and critical analyses.

Professors L. H. Van Vlack, W. C. Bigelow, and J. J. Martin members of the Doctoral Committee for their interest and advice.

To the International Nickel Company for fellowship support and in particular Mr. Donald J. Reese for his continued interest and advice.

To the Dow Metal Products Company and Mr. Jay W. Fredrickson for raw materials and chemical analyses of the magnesium rich phases.

Mr. David L. Sponseller for his assistance in the experimental phases of this program.

My fellow graduate students in Metallurgical Engineering for their cooperation, assistance, and enlightening discussions.

The Industry Program of the College of Engineering for the reproduction of this thesis.

TABLE OF CONTENTS

TABLE OF CONTENTS (CONT'D)

LIST OF TABLES

LIST OF FIGURES

LIST OF FIGURES (CONT'D)

ABSTRACT

The alkali and alkaline earth metals have been used extensively for deoxidation, desulfurization, and control of graphite shape but equilibrium data regarding their solubility in liquid iron base alloys have been unavailable because of experimental difficulties. The primary purpose of this investigation was to develop a method to measure the magnesium solubility in Fe-C-Si alloys within the ranges of 2-5% carbon and 0-3% silicon. These data are not only important from an engineering point of view in the manufacture of ductile iron, but also have several thermodynamic implications since recent predictions have been made regarding the effect of magnesium on carbon interaction parameters.

The experimental procedure is based upon selection of an open system in which the pressure of argon is controlled at a level greater than the vapor pressure of magnesium to prevent the magnesium from boiling. The equilibrium is therefore carried out in a pressure vessel in which the melt is heated by induction and sampling is accomplished by a suction technique. Both the magnesium and iron rich liquids are sampled. Mutual saturation is developed in very short times.

It has been found that the solubility of magnesium in the iron base liquid is quite appreciable (up to 3%) instead of zero as formerly supposed. The most important variables affecting solubility in order of decreasing importance are carbon content, temperature, and silicon content. The solubility of iron in the magnesium rich phase increases with temperature and probably with silicon. The maximum experimental temperature is limited to 2600°F due to chemical instability of the alumina crucibles above this temperature.

Magnesium has been found to increase the carbon solubility and give negative values to the thermodynamic interaction parameters:

$$\lambda_C^{Mg} = -\left(\frac{\partial N_C}{\partial N_{Mg}}\right)_{a_C} \qquad \zeta_C^{Mg} = \left(\frac{\partial \ln \gamma_C}{\partial N_{Mg}}\right)_{\frac{N_C}{N_{Fe}}}$$

These data do not correspond to values predicted by others based upon periodic relations among the elements. However these predictions take into account only the attraction between magnesium and carbon atoms. Another factor may be the strong repulsion between iron and magnesium atoms. A similar argument also explains the increase in magnesium solubility as the carbon and silicon are increased.

The experimental procedure employed in this investigation can be used in other liquid-liquid equilibrium studies with equivalent or lesser differences in vapor pressures of the components. The solubility data are of course important to the technology of ductile cast irons. The thermodynamic calculations on the other hand point out a non-adherence to periodic effects which may also be anticipated for other immiscible elements and suggest a modified periodicity for such systems.

INTRODUCTION

Deoxidants and desulfurizers containing alkali and alkaline earth metals have been used for many years in the treatment of liquid ferrous and non-ferrous alloys. Examples are calcium manganese silicon in steel making, magnesium additions to nickel base alloys, lithium additions to copper and sodium to aluminum alloys. More recently the development of ductile iron has been based upon the addition of magnesium to iron base alloys. In many cases these additions have been made with a scant background of information regarding the solubility of the added element in the liquid metal which is treated. Even more striking is the fact that additions have been made to alloys in which no solubility is supposed to exist, for example, magnesium to cast iron.

The reason for the scarcity of data has been that the alkali and alkaline earth metals boil off the surface of liquid iron alloys since their vapor pressures exceed atmospheric pressure at these temperatures. For example, the vapor pressure of magnesium is over 10 atmospheres in this temperature range, Figure 1.

In view of the importance of data of this type in understanding the treatment of liquid metals it was decided to develop suitable equipment for studying liquid--liquid equilibria for these alloys and then to obtain data for the Fe-C-Si-Mg system. Also in addition to their engineering significance, solubility data of this type can be used to obtain activity coefficients and other measures of atomic interactions in liquids.

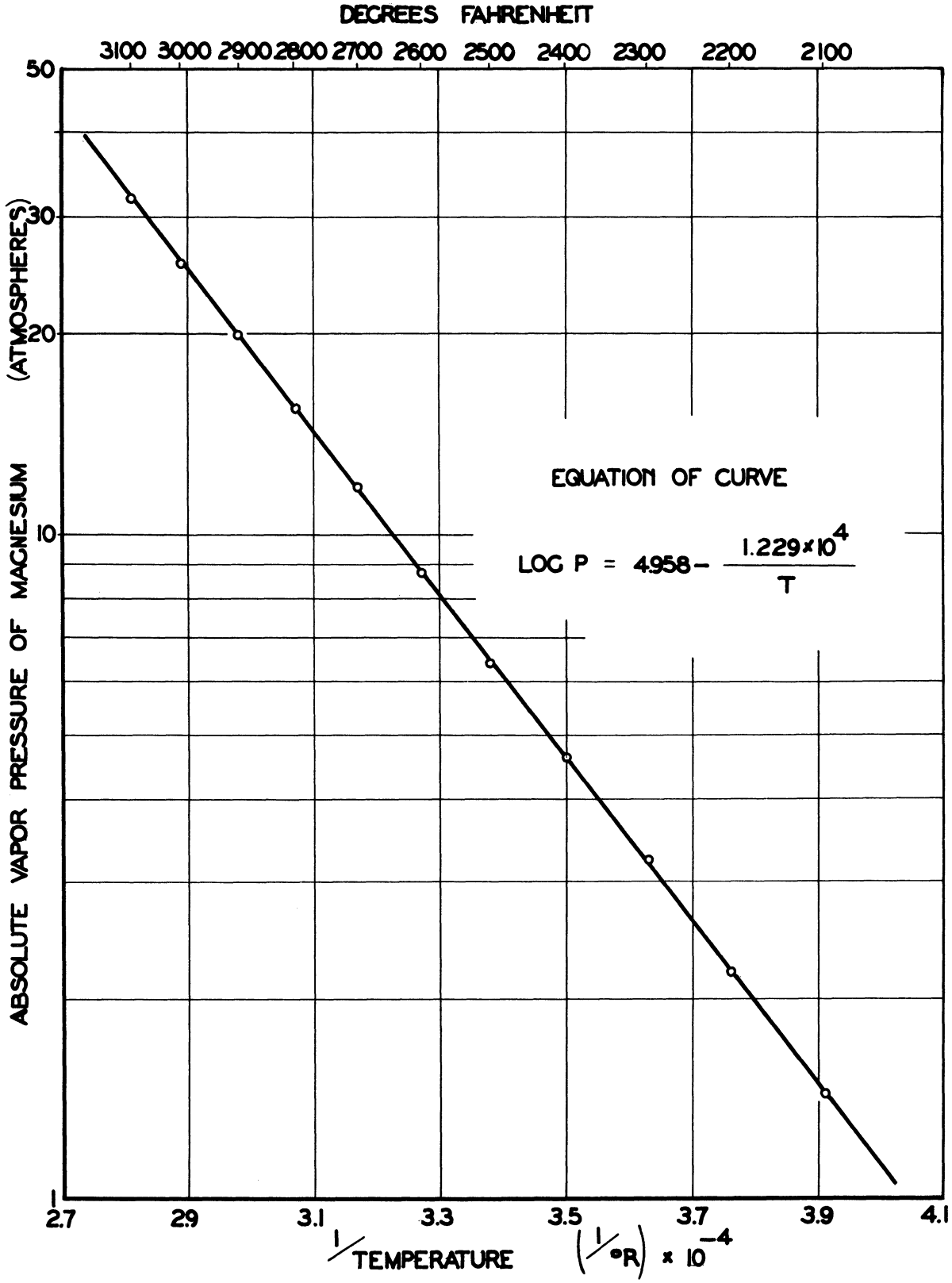

Figure 1. Variation in Vapor Pressure of Magnesium With Temperature.(26)

REVIEW OF THE LITERATURE

The literature pertinent to this investigation can be classified into two principal categories:

A. Magnesium addition to iron; non equilibrium considerations.

B. Magnesium solubility in the iron-carbon-silicon system; equilibrium considerations.

A. Magnesium Addition to Iron; Non Equilibrium Considerations

The recovery of magnesium when added to iron is generally low due to its low melting point and boiling point relative to the pouring temperatures of iron alloys. In order to improve the recovery of magnesium many methods of addition have been devised. These can be classified as transfer, injection, plunging, and pressure techniques.[1]

The transfer method which is most widely used in this country consists of adding a master alloy with a magnesium content usually less than 20% to the liquid iron. The other elements present in these alloys are usually Ni, Cu, Si, Ce, Ca, and (or) Fe. In other methods the magnesium is added in the form of a compound that will break down at high temperatures such as $MgCl_2$ or Mg_3N_2.[2,3,4] Since the manufacture of these alloys results in added expense, development work has been carried out using pure magnesium. Such methods include using magnesium chips or compacts.[5,6,7]

The injection technique consists of introducing vapors derived from metal powders and in some instances an inert gas carrier is used. However in most cases pure magnesium is used which not only is more

economical but also prevents solution of other elements as is the case when a master alloy is used.[8,9,10]

Plunging techniques have been developed as a natural consequence of trying to find a more economical method for introduction of magnesium. The magnesium can be held under the metal surface and allowed to react. The plunger usually assumes the form of an inverted graphite crucible with holes to allow the magnesium vapor to escape. In many cases the magnesium is coated with resin or similar material to reduce the volatilization rate.[1]

The most recent development is the use of a pressure vessel. The magnesium is added under pressure to counteract the high vapor pressure of magnesium at the temperatures of molten iron.[11,12,13,14,15] With the possibility of higher magnesium recovery, the treated metal can then be diluted with untreated iron which again results in better economy.

In each of the methods presented above the maximum magnesium solubility is never attained, since the conditions associated with the addition technique are non-equilibrium in nature.

B. Magnesium Solubility in the Fe-C-Si-Mg System; Equilibrium Considerations

Most of the information regarding Fe-Mg equilibrium is at the magnesium rich end of the phase diagram. Several investigators have suggested that a eutectic exists at very low iron contents in magnesium base alloys.[16,17,18,19] A.S. Yue has indicated a eutectic at 0.006 wt pct. Fe with a solid solubility of 0.001 wt. pct. Fe.[20] The eutectic temperature is very close to the melting point of pure magnesium. Equilibrium data are also available for the Mg-Si and Mg-C systems.[21,22,23]

Only fragmentary data have been published for iron rich alloys containing magnesium. Zwicker,[24] has carried out an approximate equilibrium study between magnesium vapor and a liquid iron-carbon alloy. A magnesium solubility of 0.9 wt. pct. was reported but it is questionable whether equilibrium was attained since the experimental conditions are inadequately described. Landa[25] performed microhardness surveys of solid iron-magnesium alloys and stated that from his results, considerable magnesium was retained in solid solution.

The justification for an investigation of magnesium solubility in cast irons is therefore apparent. Also further information can be obtained concerning the solubility of iron in magnesium at high temperatures.

DEVELOPMENT OF EXPERIMENTAL PROCEDURE

The investigation of the solubility of magnesium in cast iron imposes several problems which in some respects are unusual to the type of system. The difficulties are both mechanical and chemical in nature; mechanical from the standpoint of the high vapor pressures encountered; chemical from the point of view of high reactivity of superheated magnesium. Some of these problems can be minimized by a careful analysis of the experimental variables. Therefore in this section the pre-experimental analysis will be discussed before the equipment design is described.

A. Pre-Experimental Analyses

Magnesium has a melting point of 1202°F and a boiling point of 2025°F. Therefore at temperatures of molten iron alloys the vapor pressure of pure magnesium is greater than one atmosphere. The vapor pressure curve is included in Figure 1, which is derived from a least square calculation of numerical data from the University of California.[26] Since cast iron and magnesium are partially miscible, Figure 2, a choice is possible between an open or a closed system. Both of these cases can best be discussed with the aid of the phase rule. In the most general condition the phase rule is stated as:

$$V = C - P + 2$$

where P = the number of phases in equilibrium

V = variance or degrees of freedom

C = the number of components

The number 2 refers to temperature and pressure

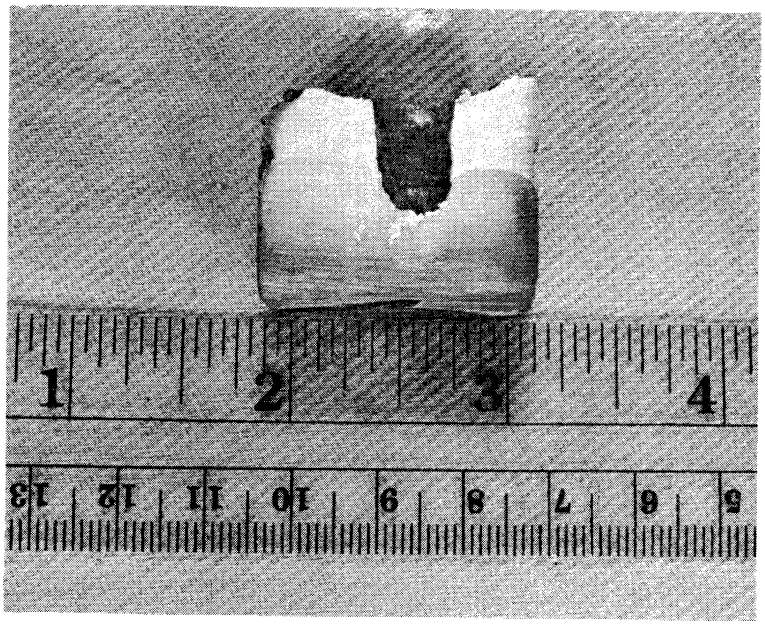

Figure 2. Photograph of Iron Rich and Magnesium Rich Layers of an Fe-C-Mg Melt. Melt allowed to solidify in place. Note presence of two layers and cavity formed by thermocouple tube.

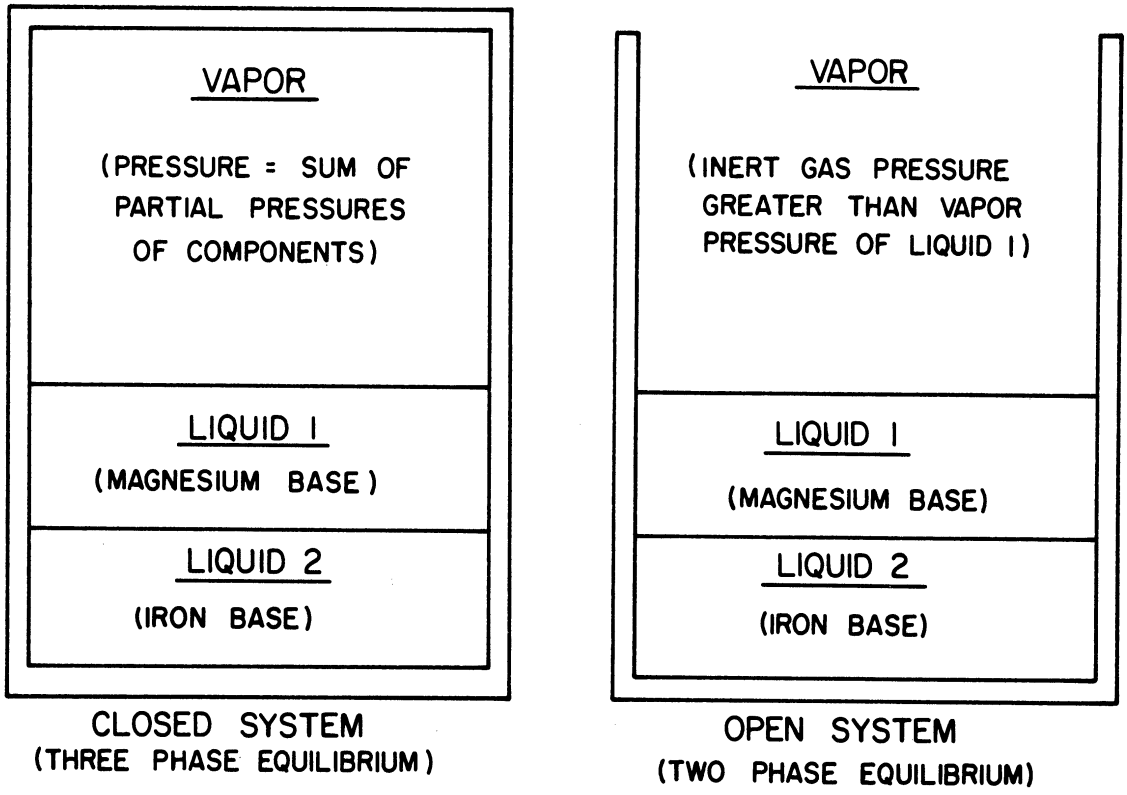

Figure 3. Diagrammatic Sketch of Closed and Open Systems in Fe-Mg Equilibrium.

Another equation which can be of use involves the phase variables U and the number of chemical species N:

$$U = P(N-1) + 2$$

As outlined by Case[27] a relationship exists between the number of components and chemical species:

$$C = N - E$$

where E = the number of independent relations among the concentration variables, i. e., mass action equilibria.

However for the present analysis $E = 0$ and $C = N$.

1. Closed System

A closed system would consist of three phase equilibrium: an iron base liquid, a magnesium base liquid, and a gas, Figure 3. Therefore for the Fe-Mg system ($C = N = 2$):

$$U = P(N-1) + 2 = 3(2-1) + 2 = 5$$

or as an example the phase variables stated could be: percent magnesium in liquid 1, liquid 2, and gas plus temperature and pressure. The phase rule predicts the number of degrees of freedom to be:

$$V = C - P + 2 = 2 - 3 + 2 = 1$$

This means that if any one of the phase variables such as temperature is experimentally fixed the other four variables such as mole fractions in the three phases and pressure are also fixed. Although a two component system has been considered (Fe-Mg), the addition of more components merely increases the number of phase variables and number of degrees of freedom. The net result is that for more components, more of the phase variables must be fixed experimentally. This is usually done

by adding a definite amount of the new component which leads to definite amounts in each of the phases according to the partition factor at temperature. The end result is that only temperature remains to be altered.

There are several experimental difficulties encountered in a closed system which are not readily apparent in the simplicity of the phase analysis. First, a container must be available which will be able to withstand the high pressures and chemical reactivity of magnesium. The container must also be kept at the same temperature over its entire surface to prevent condensation and the introduction of another phase. However, the most difficult problem is to sample the liquids at a given temperature as this is the object of the study and the compositions of the liquid are a function of the temperature. Therefore, the magnesium content in iron of a slowly cooled sample might be expected to be lower and not indicative of the solubility at the temperature where the three phase equilibrium had been established.

Because of these problems a natural choice is to consider an open system where the difficulties can be largely overcome.

2. Open System

A special type of open system is chosen such that an inert gas (argon) is supplied at a pressure which is greater than the vapor pressure of magnesium at a given temperature, Figure 3. This in effect prevents the magnesium from boiling. The phase analysis then depends upon the following assumptions:

1. Only the two liquid phases enter into the equilibrium and equilibrium can be established as long as two liquids are maintained, Figure 2.

2. Argon does not enter into the equilibrium as it is insoluble in both liquid phases (just as air is neglected in normal metallic phase systems).

3. Pressure has no effect on the liquid-liquid equilibrium except for possible kinetic factors. It is generally accepted that the effect of pressure is merely to produce more intimate contact between the two liquid layers. This problem was however investigated experimentally as discussed later.

Therefore, since there are only two phases at equilibrium and pressure is not a variable, the phase analysis for Fe-Mg becomes:

$$U = P(N-1) + 1 = 2(2-1) + 1 = 3$$

and

$$V = C - P + 1 = 2 - 2 + 1 = 1$$

The phase variables can then be considered as mole fraction magnesium in each liquid plus temperature, while the magnesium solubility can be most readily fixed by the temperature. The addition of another element or component again results in the necessity of fixing another phase variable. As an example in the Fe-C-Mg system the phase variables can most readily be fixed by the carbon content and temperature.

It is interesting to note that the choice of a open system results in the same number of degrees of freedom as a closed system for the same number of components.

B. Experimental Technique

1. Operation of the Equipment

Since an argon atmosphere is used to prevent boiling of the magnesium, it is necessary to provide sealed equipment capable of manipulation by external controls. The pressure vessel, Figure 4, has been designed for an operating pressure of 500 psi and is constructed of austenitic stainless steel. More specific information as to design and materials is included in the Appendix. Suitable safety devices are provided to prevent excessive internal pressures. Also the inside of the vessel is clad with a copper sheet to which water cooled copper tubing is soldered in order to prevent overheating of the walls from radiation and induced currents.

The temperature of the melt is controlled by a 50 kw 3000 cycle motor generator set which heats both a graphite susceptor and the melt itself. The susceptor provides a constant temperature chamber, Figure 5. The thickness of the susceptor is such that roughly one-half of the current is induced in it while some current is also induced in the metal charge.[28] Figure 6 shows the coil, crucible, charge, susceptor, and refractories for the basic heating unit. Figure 7 is a cross-sectional drawing of the same unit.

In order to sample the melt, the crucible is lowered out of the coil by external controls and swung under the sampler which draws up specimens for chemical analysis, Figure 8 and 9. The positions of the various internal components (heating unit, sampling device, and turning mechanism) are indicated in Figures 10 and 11.

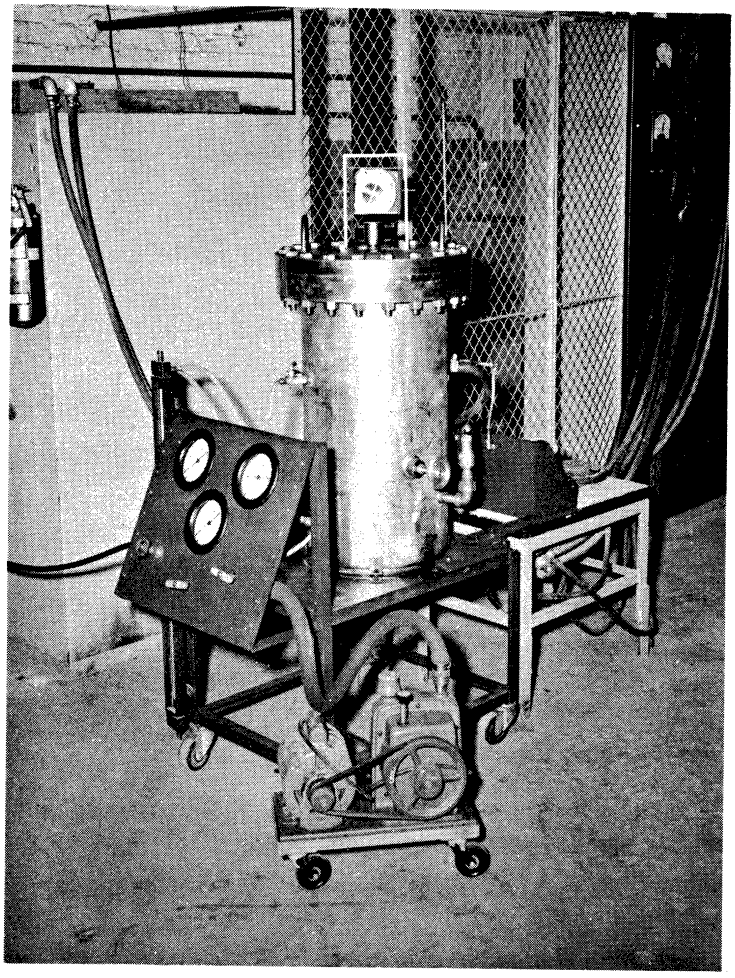

Figure 4. Overall View of Pressure Vessel with Control Equipment.

Figure 5. Graphite Susceptor Which Forms A Heating Chamber of Uniform Temperature.

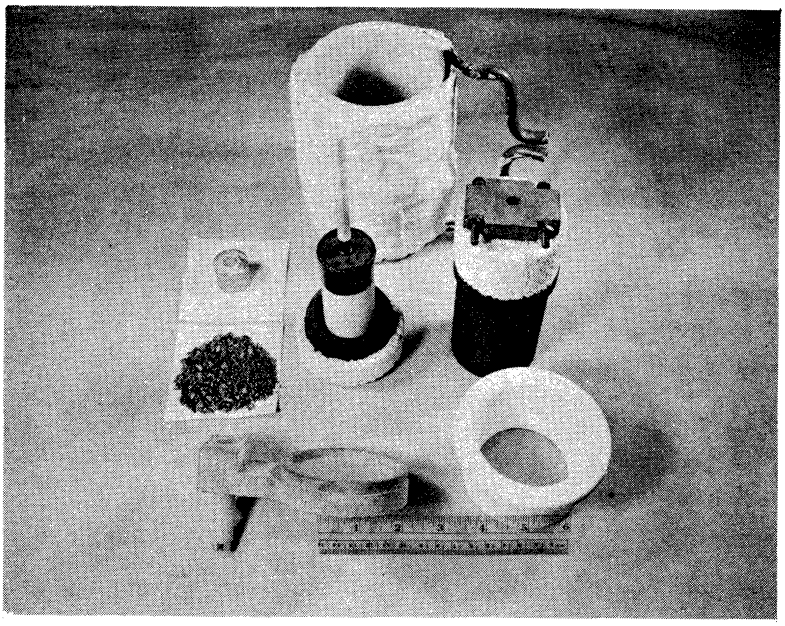

Figure 6. Disassembled Heating Unit, Crucible, Susceptor, and Metal Charge Removed From Pressure Vessel.

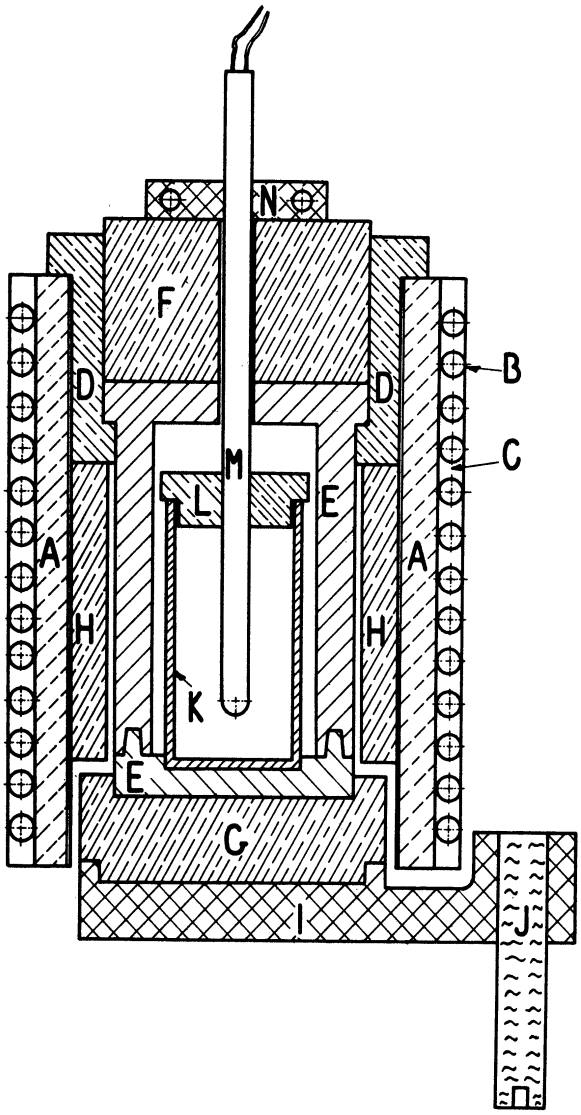

A. Fused silica coil form coated on inside with Sauereisen cement plus TiO_2.
B. 1/4" copper tubing - 13 turns.
C. Sauereisen cement coating over coil.
D. Alumina hanger for graphite susceptor.
E. Graphite susceptor.
F. Upper alumina insulation brick.
G. Lower alumina insulation brick.
H. Alumina insulator to reduce graphite radiation.
I. Transite Platform.
J. Nylon rod to turn platform.
K. Crucible (alumina or graphite).
L. Crucible cover (alumina or graphite).
M. Alumina thermocouple protection tube.
N. Spring clamp of transite to retain thermocouple protection tube when crucible is lowered.

Figure 7. Cross Section of the Assembled Heating Chamber.

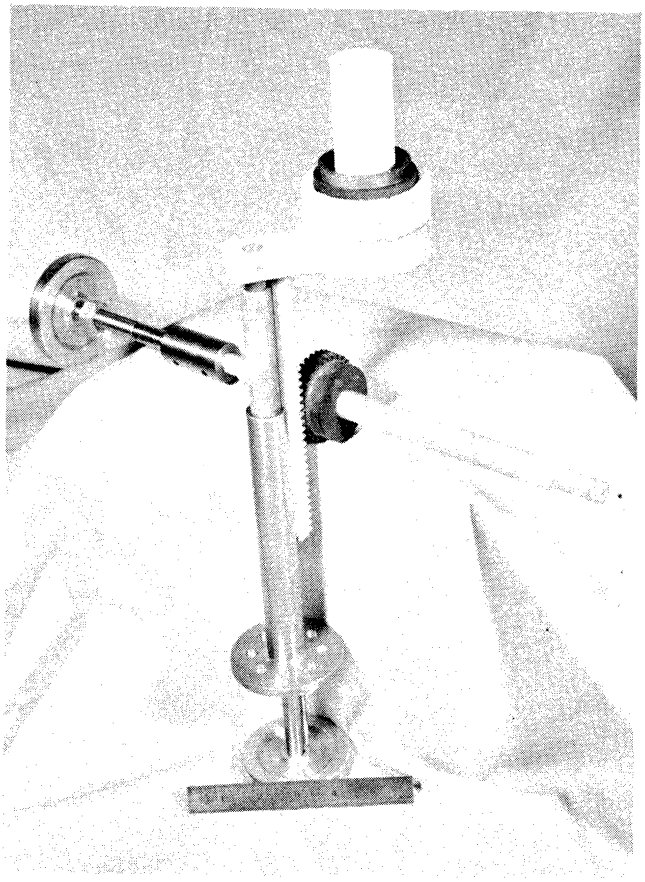

Figure 8. Lowering and Turning Mechanism Removed from the Pressure Vessel.

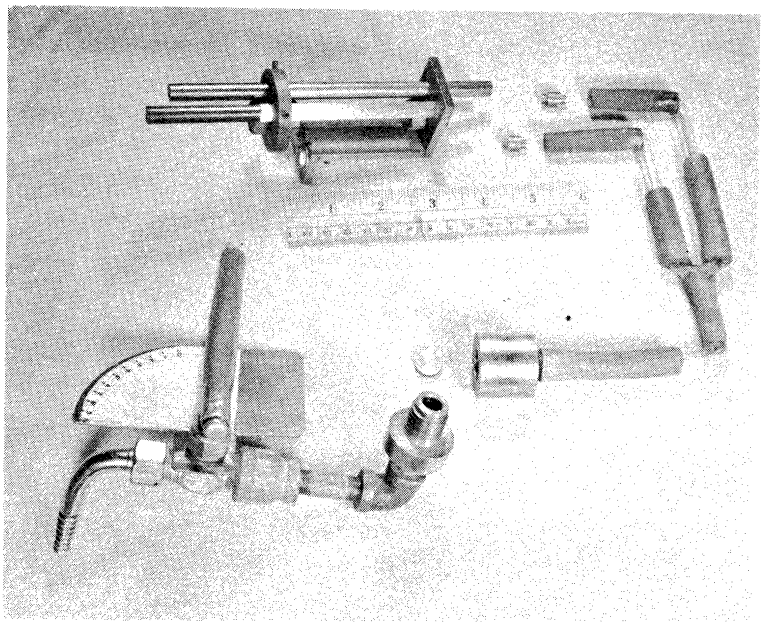

Figure 9. Disassembled Sampling Device, Orifice, and Outer Needle Valve.

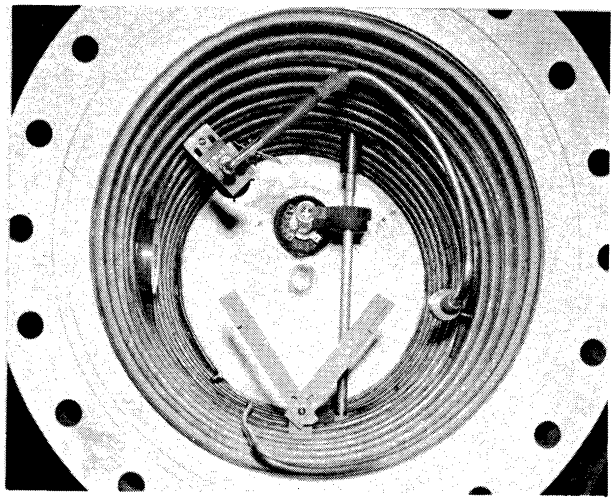

Figure 10. Top View of Pressure Chamber with Cover Off and Turning Mechanism and Sampling Device in Place.

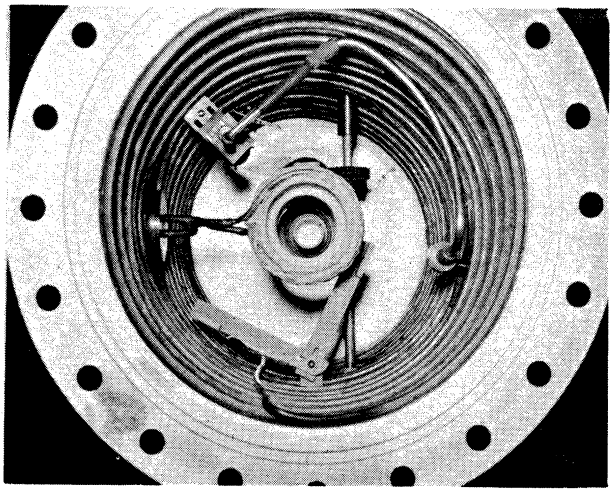

Figure 11. Top View - Same as Figure 10 except coil and Crucible are also in place.

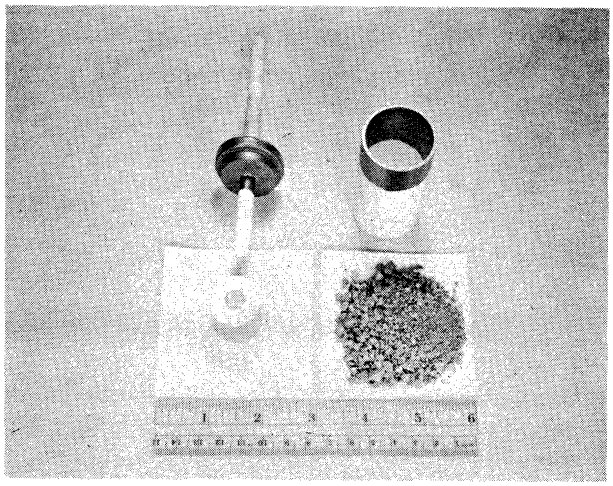

Figure 12. Crucible, Thermocouple Protection Tube with Attached Cover, and Raw Metal Additions.

The metal charge consists of approximately equal metal volumes, 75 gms of ferrous material and 15 gms of magnesium, Figure 12. In the case of a carbon saturated melt the crucible and cover are graphite while all other heats employ an alumina crucible and cover. After the solid charge is placed in the crucible and the alumina thermocouple protection tube with attached cover is in position, the unit is placed in the graphite susceptor within the coil, Figure 7. The thermocouple and sampling device are inserted and the vessel lid is secured. In all cases "O" rings are used in movable joints and entrance ports, such as around the coil leads, to insure pressure tightness.

The entire pressure vessel is evacuated twice and then argon is introduced. The argon pressure is chosen at one and one-half times the absolute vapor pressure of pure magnesium at the temperature of the experiment as indicated in Figure 1.

The temperature of the melt is indicated on a strip chart recorder and maintained at $\pm 5\,^{\circ}F$ of the desired temperature. Before each heat the recorder accuracy is checked against that of a precision potentiometer. There has been no experimental evidence of induced currents in the thermocouple. After holding the melt for 5-10 minutes at temperature, the crucible and susceptor are lowered out of the coil and positioned beneath the sampling device, Figures 7, 8, 9, and 10. The time interval until sampling is started varies from eight to ten seconds.

The sampling device consists essentially of two tubes which can be exhausted to the atmosphere outside of the vessel. The tubes are of different lengths such that one tube is in the iron base liquid and the other in the magnesium base liquid. Samples are taken by releasing some

of the argon from the tubes so that the pressure differential between the melt and the interior of the tubes forces the liquid metals up the tubes and rapid freezing occurs, Figure 13. The amount of argon to be released is dependent upon the operating pressure and is controlled by passing the argon through a flowmeter. The flowrate necessary to provide sound samples is pre-determined by experiment. The samples can then be readily analyzed chemically. It should be mentioned that expansion of the argon gas within the iron liquid sample tube prevents pick-up of magnesium when it pierces the magnesium base liquid.

2. Raw Materials

The iron base material is pre-melted in an argon atmosphere and cast into a shape which conforms to that of the crucible. These shapes have been produced in 2, 3, and 4.3% C levels; intermediate carbon levels are obtained by crushing the piece and adding spectrographic grade carbon. Exclusive of carbon, the chemical compositions are given below in wt. pct. (elements of most importance):

Si	Mn	P	S	Cr	Ni	Cu	Al
< 0.03	0.001	0.002	0.005	< 0.01	0.035	0.01	< 0.003

The magnesium was supplied by the Dow Metal Products Company as sublimed and extruded to one inch rounds. A representative analysis of this grade of material is (parts per million):

Al	Fe	Mn	Ni	Pb	Zn	Si
3.5	7	18	3	5	100	100

The silicon used for additions was 99.9% Si with iron as the major impurity.

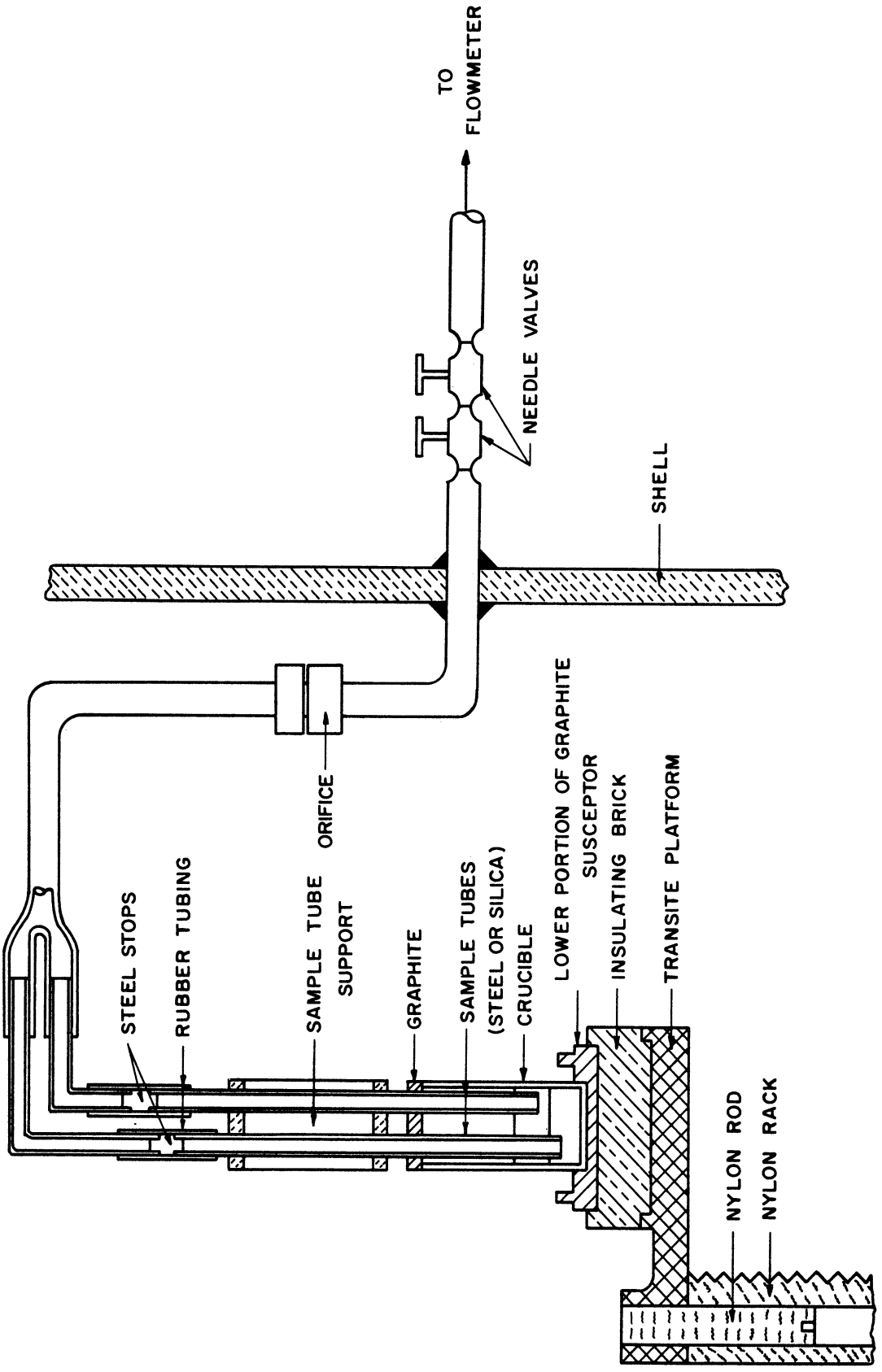

Figure 13. Cross Section of the Sampling Sequence with the Crucible in Position

C. Evaluation of Experimental Procedure

In view of the rather new techniques involved it was considered essential to explore the effects of several variables before attempting to investigate the Fe-C-Si-Mg system itself. The conditions requiring evaluations were the effects of pressure, sampling time, time required at temperature to attain equilibrium, and contamination from the crucible and these may be discussed in this order.

1. Effect of Pressure

A series of melts was prepared at 2250°F in which the argon pressure was controlled at from 2 to 8 times the gauge vapor pressure of pure magnesium. The results were:

%C	% Mg	Argon Pressure
4.22	1.34	60 psig
4.29	1.39	120 psig
4.27	1.38	240 psig

(balance Fe in all cases)

The reason for the slight variation in magnesium content can be explained by errors in analysis and secondly by the carbon content. (As will be pointed out later, an increase in carbon is accompanied by an increase in magnesium). Therefore, the only requirement for the applied external pressure is that it be great enought to prevent losses of the magnesium layer by boiling.

2. Effect of Time to Sample and Representative Samples

Figure 14 shows the effect of time to sample on the magnesium content of an iron containing 4.22% C. The decrease in magnesium content with time is due to cooling of the melt (lower temperatures result in lower solubilities). It is interesting to note that an extrapolation to time zero results in very little difference in magnesium solubility when compared to the 10 second value. Therefore, even though the melt cools approximately 50°F in the 10 second interval required to sample, the kinetics of magnesium rejection are such that the samples are still representative of the holding temperature of 2250°F. It is of course conceivable that a variation in the absolute value of magnesium may lead to variation in this sampling error.

The laboratory performing the chemical analyses on magnesium in the iron base liquid lists the accuracy at approximately $\pm$ 5% of the amount analyzed. However, the analysis of a normal heat consists of taking two specimens from the drawn samples with duplicate analyses conducted on each specimen. The results are then averaged and it is believed the accuracy is approximately $\pm$ 2% of the amount analyzed since the reproducibility from one heat to another is of this order of magnitude.

On the other hand the analyses for iron in the magnesium base liquid are subject to a larger degree of error. The major problem is in removing approximately 1000°F superheat from the magnesium before an iron rich phase settles out due to its greater density. Therefore only the very upper sections of the samples freeze rapidly enough to be considered representative of the liquid equilibrium. As an example, the

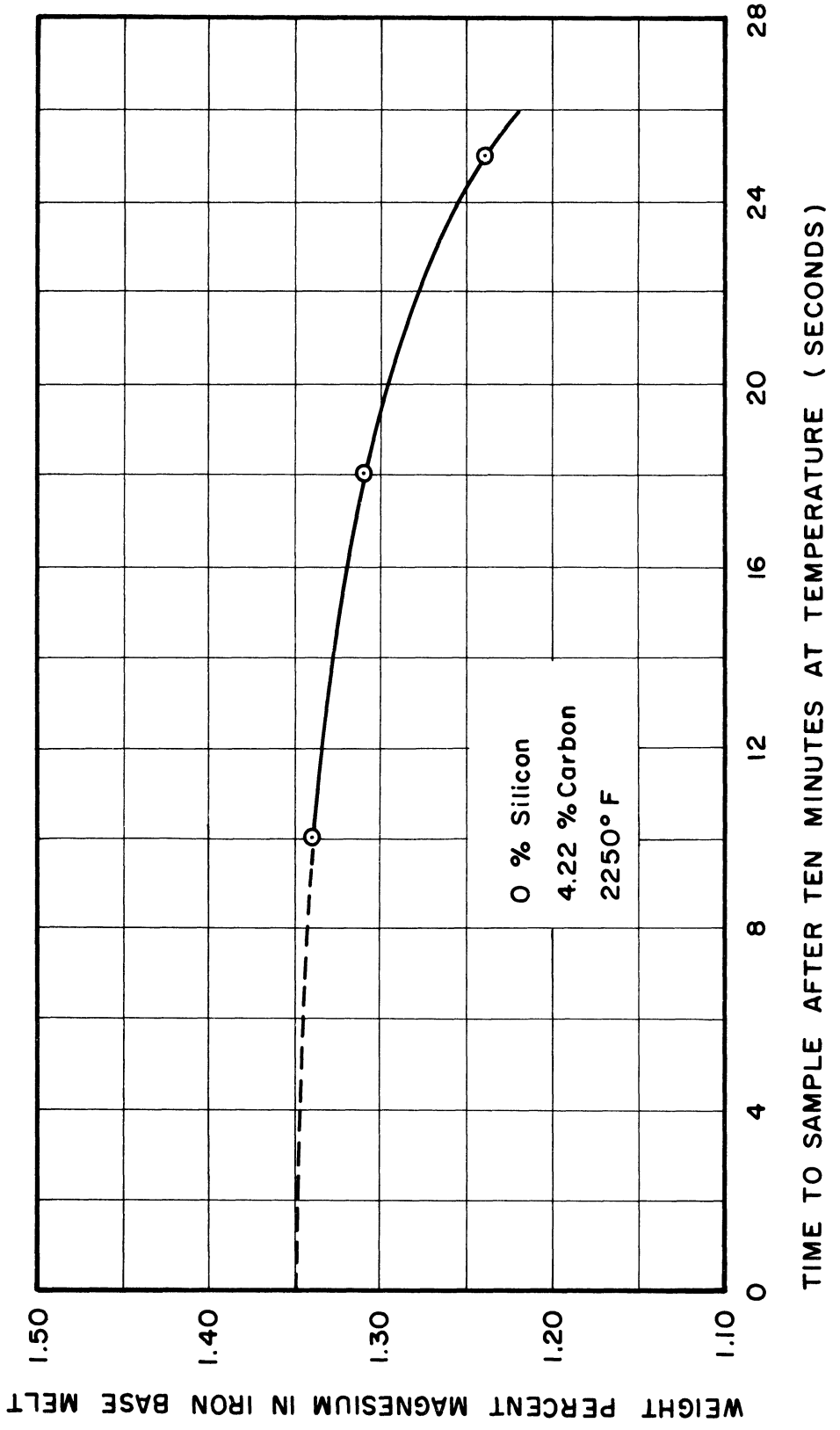

Figure 14. Effect of Time Delay Before Sampling on Solubility of Magnesium in the Iron Rich Liquid.

iron content might be 2% at the top and as much as 20% at the bottom where it has settled out. As might be expected the higher sampling temperatures result in a greater difference between iron contents at the top and bottom of the samples. This large deviation is not present in the iron base samples as the superheat is much less. The iron contents listed for the magnesium layer are therefore not of the same accuracy as the magnesium contents in the iron base liquid, although the solubility data do not indicate a severe scatter of points.

3. Effect of Time at Temperature

The establishment of dynamic equilibrium is indicated by Figure 15. The criterion for dynamic equilibrium is that the magnesium content remain substantially constant as the time of holding is increased. It can be seen that five minutes at temperature is more than enough to establish dynamic equilibrium. In fact a sample taken just after the temperature has been attained is very close to the equilibrium value. In most instances a ten minute period at temperature is followed as the standard procedure although at 2600°F only five minutes is used preceded by five minutes at 2450°F in order to reduce the alumina reduction by the molten magnesium. This effect is considered in more detail under "crucible contamination."

The time to melt a 4.3% C iron-magnesium mixture is approximately 20 minutes (2050°F). The next 200°F increase in temperature takes about 3 minutes which means that equilibrium in the liquid state is being established while heating. As has been previously mentioned, some current is induced in the melt or in other words magnetic stirring probably assists this rapid approach to equilibrium.

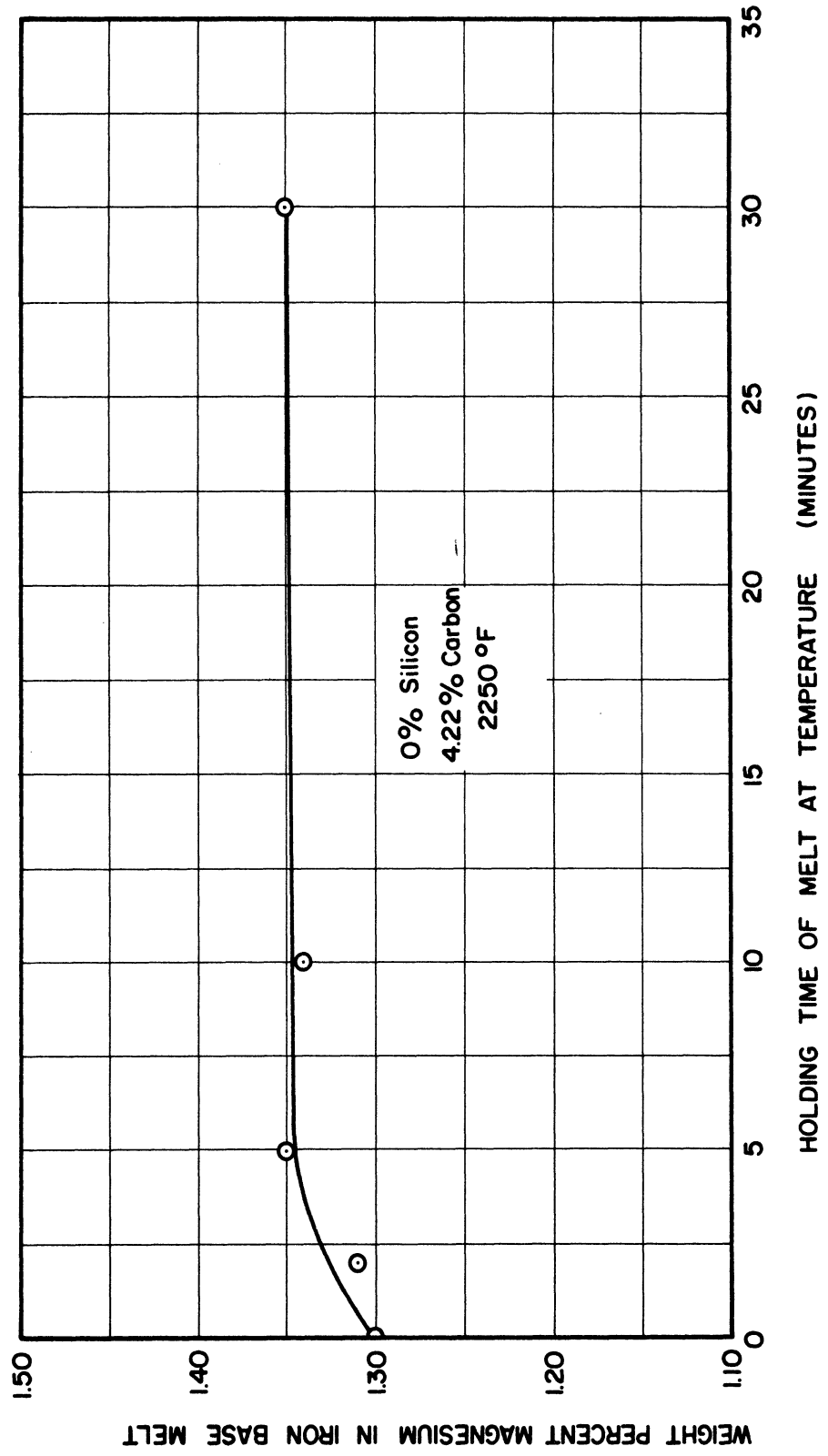

Figure 15. Effect of Time at Temperature Upon the Solubility of Magnesium in the Iron Rich Phase.

4. Effect of Contamination from the Crucible

It should be pointed out that 2600°F has been the highest temperature investigated. The principal interest in higher temperatures would be to investigate the lower carbon levels which could not be attained due to the requirement of 100°F superheat to sample at 2600°F. The lower carbon levels would of course result in lower magnesium solubilities, which somewhat reduces the interest in this portion of the solubility curves.

In general, the selection of a refractory for a crucible material is based upon chemical, thermal, and mechanical stability. In the present consideration of a container for highly superheated magnesium, chemical stability becomes the most difficult problem to solve.

A large number of commercially available crucibles has been tested for reaction with molten magnesium at temperatures in excess of 2000°F (Various grades of Al_2O_3, MgO, and ThO_2). In general even the so-called high purity grades of MgO and ThO_2 cannot be used since they usually contain impurities which are readily leached out by magnesium, notably SiO_2. The other more common oxides are also generally not considered since their free energy of formation is greater than that of MgO. Non-oxide refractories such as the nitrides and carbides have also been synthesized into shapes which could be tested for chemical stability. The most promising of these at the moment appears to be titanium nitride (TiN), however, it is difficult to sinter a crucible to low porosity levels.

It will be recalled that alumina has been selected as the crucible material for heats other than the graphite saturated melts. The alumina should be thermodynamically unstable to magnesium. However, the alumina grade used in this study is of high purity and of very high density. Since the reaction rate is dependent upon the exposed surface area, the low porosity leads to relatively low reaction rates. As an example the aluminum content of the iron layer varies from 0.03 wt. pct. at 2300°F to 0.15 wt. pct. at 2600°F. An increase of another 150°F to 2750°F results in an aluminum content in excess of 1.0 wt. pct. It has been noted that a definite aluminum partition exists between the iron and magnesium base melts with an approximately constant ratio of

$$\frac{N_{Al} \text{ in Fe}}{N_{Al} \text{ in Mg}} = 10 \ .$$

Due to the fact that the activity of aluminum must be the same in each liquid, the inverse ratio exists between the activity coefficients or

$$\frac{\gamma_{Al} \text{ in Mg}}{\gamma_{Al} \text{ in Fe}} = 10 \quad \text{where} \quad a_{Al} = N_{Al}\gamma_{Al} \ .$$

The activity coefficient of aluminum in iron-carbon alloys can be readily calculated from the data of Ohtani and Gokcen,[30] which refers to temperatures of approximately 2900°F. However, even though the actual temperatures are lower and the ratio as given is probably dependent upon carbon concentration, it is interesting to note that γ_{Al} in Mg is fairly close to one. The same general conclusion can be reached from the extrapolated data of Schneider and Stoll[29] where the heats of mixing and activities of magnesium in the Al-Mg system are given for lower temperatures.

The aluminum content of the iron rich layer will probably have an effect on the magnesium and carbon solubility as presented. However, it is believed this effect is not large due to the relatively small amounts of aluminum present. This conclusion is also not without some experimental justification. As an example, Figure 15 (time of holding a melt at 2250°F) shows very little change in magnesium solubility between 5 and 30 minutes although the aluminum content after 30 minutes would be greater. Also Figure 16 (effect of temperature and carbon on magnesium solubility) shows roughly the same increment of magnesium solubility for 150°F intervals even though the aluminum content increases in the interval. If the effect of aluminum is significant, the 2600°F solubility curve should be displaced upward since as a first approximation the activity coefficients indicate a greater affinity between aluminum and magnesium as compared to iron and magnesium.

Although the aluminum content may be considered negligible at temperatures up to 2600°F, this temperature appears to be the upper limit for high purity alumina refractories in contact with magnesium. As previously mentioned, the development of TiN as a crucible is in process and may ultimately permit investigations of higher temperatures.

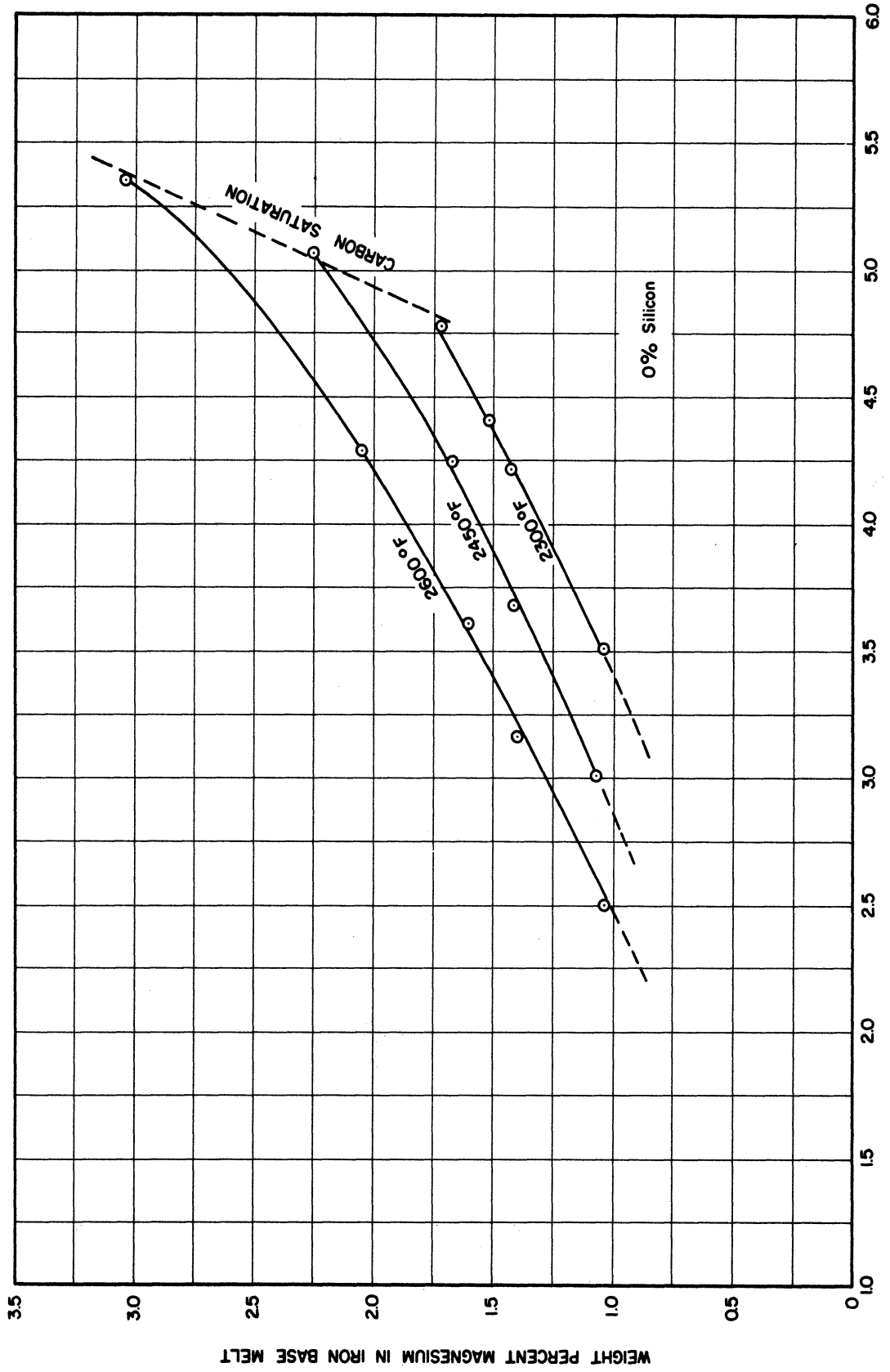

Figure 16. Effects of Carbon Content and Temperature upon the Magnesium Solubility.

RESULTS AND DISCUSSION

The detailed results of this investigation and their discussion are presented in the following major categories: A - Solubility relations, and B - Thermodynamic interactions.

A. Solubility Relations in the Fe-C-Si-Mg System

In the discussion of these results the effects of temperature, carbon, and silicon may be considered first for the iron and then for the magnesium rich layer. Following this the reactions among elements affecting solubility, the observation of phases in the solid samples, and engineering applications can be discussed. The chemical analyses of heats used in the solubility investigation are included in Table I.

1. Liquid-Liquid Data

a. The Iron Rich Phase - Effects of Temperature, Carbon, and Silicon Upon Magnesium Content

As expected, increased temperature leads to higher solubility of magnesium for all analyses investigated, Figure 16. An increase in temperature from 2300°F to 2600°F leads to an increment of about 0.5% in magnesium solubility.

The pronounced effect of carbon in raising the solubility of magnesium is quite surprising, Figure 16. An increase in 1% carbon is as effective as raising the temperature 300°F. In other words, the dissolved magnesium is increased 0.5% with an increase of 1% carbon. The maximum solubility of magnesium at any temperature is limited by the maximum amount of carbon present (carbon saturation). The lower limit

TABLE I

CHEMICAL ANALYSES OF HEATS IN EQUILIBRIUM STUDY

Heat No.	Temperature (°F)	Iron Base Melt (wt %)			Magnesium Base Melt (wt %)	
		%C	%Si	%Mg	%Si	%Fe
CSM-50	2300	4.31	0.69	1.56	0.03	1.40
CM-52	2450	4.49	*	*	nil	1.80
CM-57	2450	3.01	nil	1.07	*	*
CM-58	2600	3.61	nil	1.60	nil	2.34
CM-60	2300	4.41	nil	1.51	nil	1.43
CM-61	2600	4.29	nil	2.05	nil	2.48
CM-63	2600	3.16	nil	1.40	nil	2.06
CM-64	2600	2.48	nil	1.11	nil	1.88
CM-66	2300	3.51	nil	1.04	nil	1.30
CM-67	2450	3.68	nil	1.41	nil	1.62
CMT-68	2300	4.78	nil	1.71	nil	1.46
CSM-69	2600	2.38	0.66	1.18	0.03	2.45
CSM-70	2300	3.53	0.51	1.12	0.02	1.25
CSM-71	2300	3.02	2.80	1.07	0.10	1.14
CSM-72	2600	2.12	2.87	1.46	0.15	2.54
CMT-73	2600	5.35	nil	3.03	*	*
CM-74	2450	4.25	nil	1.67	nil	1.80
CSMT-75	2300	4.65	0.50	1.76	0.02	1.31
CSMT-76	2300	3.87	2.87	1.50	0.12	1.27
CSMT-78	2600	4.40	2.82	2.56	*	*
CM-79	2300	4.22	nil	1.43	*	*
CMT-80	2450	5.07	nil	2.25	nil	2.00
CSMT-81	2600	5.07	0.68	2.80	*	*

* Data not taken

is also indirectly controlled by the carbon content due to the necessity of approximately 100°F superheat for sampling by the suction technique. The exact amount of superheat is indeterminate as the effect of magnesium on the liquidus is unknown.

The effect of silicon is less than that of carbon as indicated by Figure 17. An increase of 3% silicon is required to obtain an increment of 0.5% magnesium solubility at 2600°F. The effect is even less at 2300°F. This is rather surprising in view of the use of silicon as an alloy base for magnesium bearing ladle additions.

If maximum magnesium content is desired in an iron base alloy at a given temperature the silicon should be omitted. The reason is that the carbon content is three times as effective as silicon in improving the solubility of magnesium. As silicon is added the amount of carbon which can be dissolved at a given temperature is reduced according to the well known effect upon the liquidus surface in the iron-carbon-silicon system. This reduction in carbon offsets the gain in magnesium solubility caused by silicon.

b. The Magnesium Rich Phase-Effects of Temperature, Carbon and Silicon Upon Iron Content

The data for this layer are not as accurate as those for the iron rich layer, first because of segregation due to the high superheat and secondly because of difficulties in determining small amounts of carbon. Subject to these qualifications the data of Figures 18 and 19 may be examined.

The solubility of iron in magnesium increases with temperature as would be expected, and is about the same order of magnitude as the

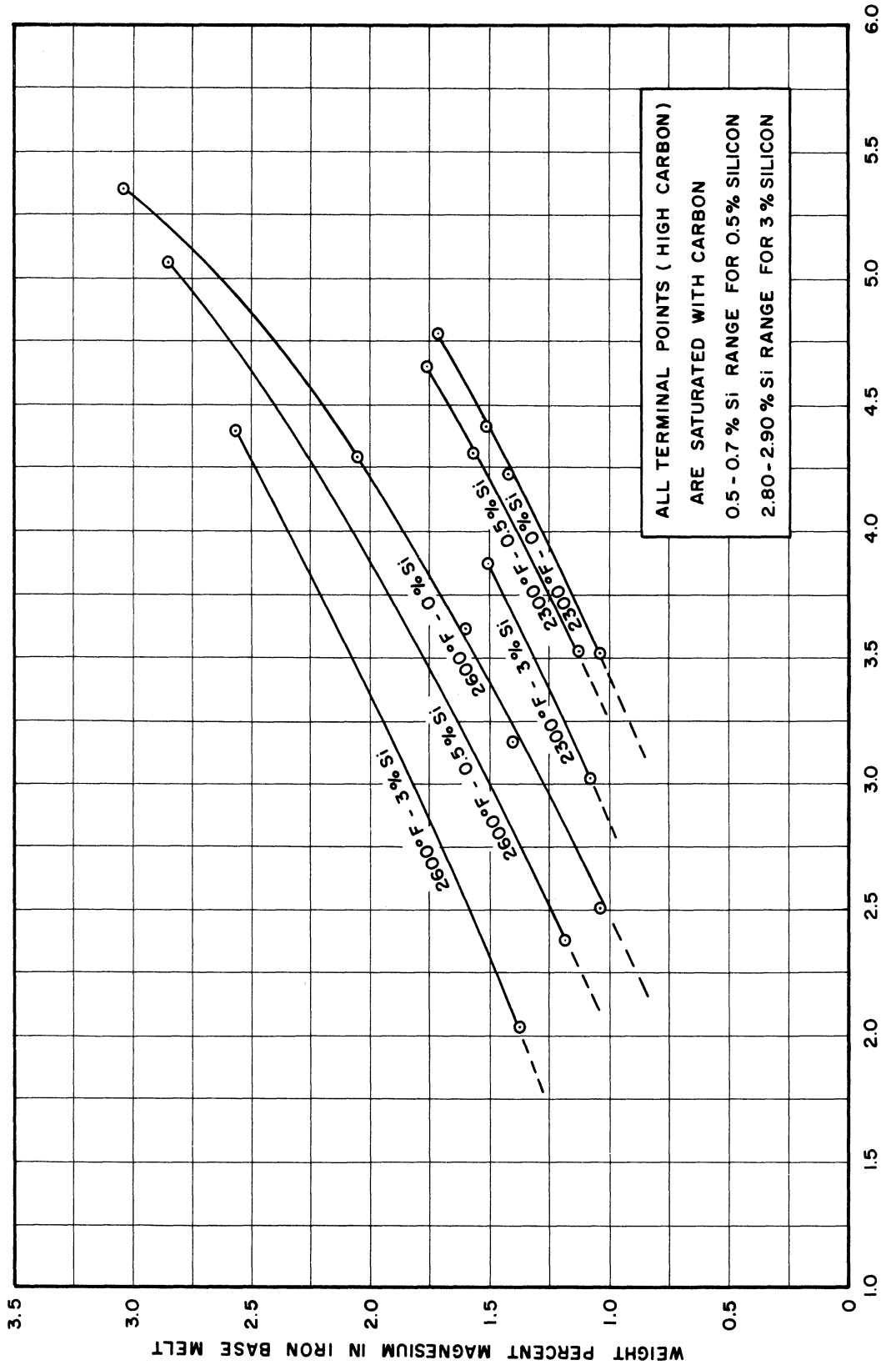

Figure 17. Effects of Carbon Content, Temperature, and Silicon Content Upon the Magnesium Solubility.

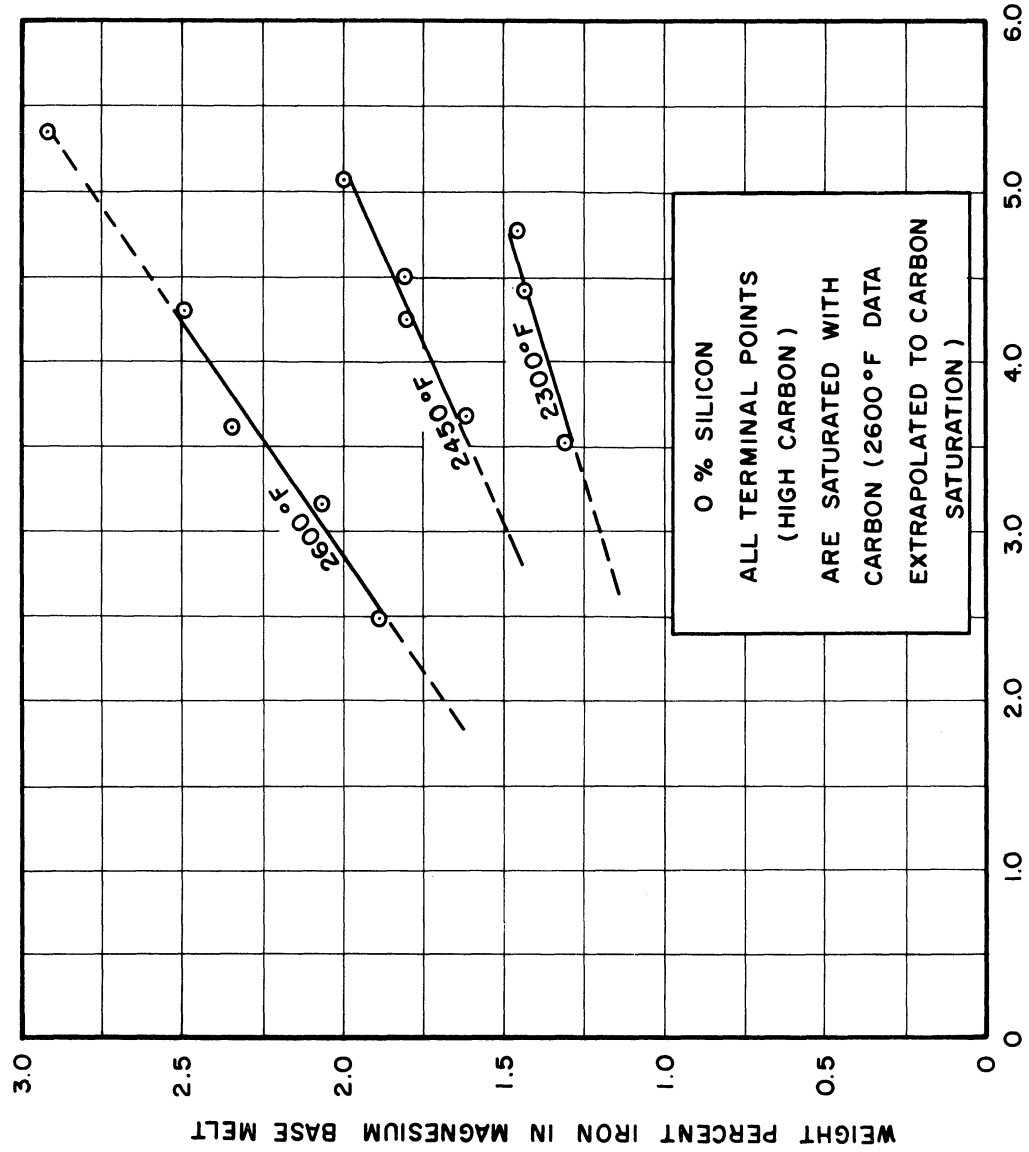

Figure 18. Iron Solubility in Magnesium as a Function of Temperature and Carbon Content of the Iron Base Liquid.

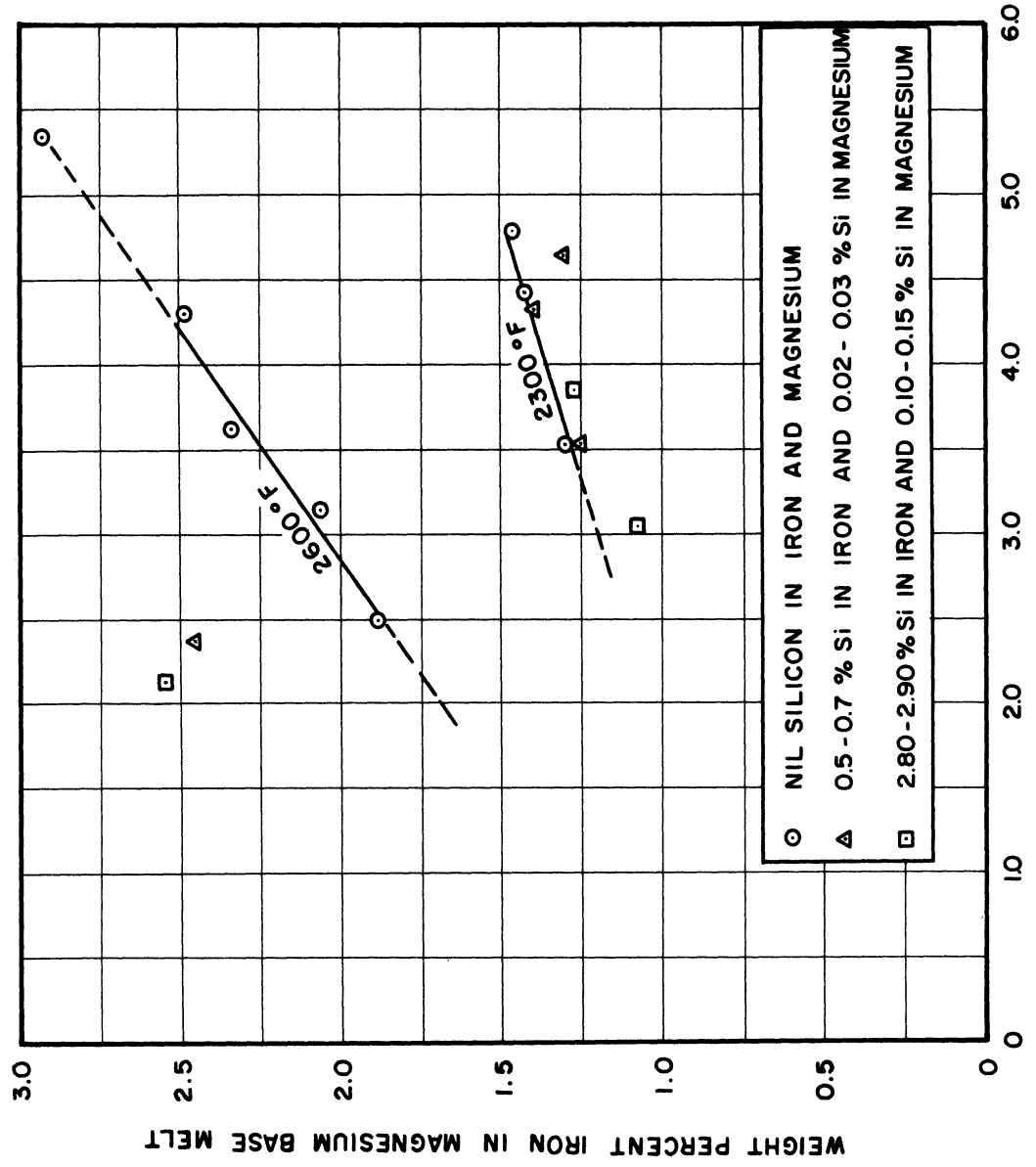

Figure 19. Iron Solubility in Magnesium as Affected by the Silicon Content.

solubility of magnesium in iron. An increase in temperature of 300°F leads to a rise of from 0.7 to 1.2% iron. These values for solubility provide an interesting extension of the data of other investigators at much lower temperatures and in the absence of carbon.

It should be noted that the iron solubility increases with the carbon content of the iron base liquid. This obviously means that carbon is present in the magnesium base melt. (This is confirmed by the examination of the solid specimens described later.) Also it has been pointed out that sampling of the magnesium base liquid is extremely difficult in that only a small sample is considered representative for iron analyses. Since it is virtually impossible to obtain a good analysis for both iron and carbon because of small samples, the iron analysis is taken as the most important. However equilibrium considerations require the carbon content in the magnesium to be dependent upon the carbon content of the iron base liquid (equal activities in both liquids at equilibrium). Therefore the carbon in iron is chosen as the most readily controllable phase variable.

The effect of silicon upon the solubility of iron is slight if real at all. The two points at 2600°F in Figure 19 indicate an effect, but the greater the superheat the larger the sampling error to be expected. However, it is felt the position of the points cannot be completely attributed to experimental error. It seems more plausible that the effect of silicon is small at 2300°F but becomes more significant at 2600°F. The degree of increased solubility is, however, not precisely determined by the position of the points in Figure 19, which merely indicates a trend.

The partition of silicon between the iron and magnesium rich layers is surprising. The data indicate a factor

$$\frac{N_{Si \text{ in Fe}}}{N_{Si \text{ in Mg}}} = 50 \quad .$$

It would be expected then that a high silicon content in the iron rich melt would not result in a large effect upon solubilities of other elements in the magnesium rich melt. Of course, it is appreciated that the activity of silicon in both layers must be the same at equilibrium, therefore

$$\frac{\gamma_{Si \text{ in Mg}}}{\gamma_{Si \text{ in Fe}}} = 50 \qquad \text{where} \quad a_{Si} = N_{Si}\gamma_{Si} \ .$$

Although the numerical values of these activity coefficients are difficult to evaluate, the well known negative deviation from Raoult's Law for silicon in iron is certainly more negative than for silicon in magnesium. This is somewhat surprising since Mg_2Si is thought to be a fairly stable compound. (ΔF_f^o = - 15,000 cal/mole at 2000°F).[22]

2. Interrelations of Effects of Elements Upon Solubilities

It is interesting to consider the solubility data from another aspect; the effect of third and fourth elements upon binary solubility relations. For example, the effects of magnesium and silicon upon the solubility of carbon in iron may be considered. Several investigators have established the graphite solubility in iron-carbon alloys as a function of temperature with good experimental agreement.[30,31,32] In the present investigation, the data of Turkdogan and Leake are used for the graphite solubility which is governed by the equation:[31]

$$\log_{10} N_C = - \frac{560}{T} - 0.375$$

where N_C = mole fraction of carbon and T is in °K.
From this relation the carbon content at saturation may be calculated for 2300-2600°F as shown in Table II.

It has also been suggested[30,31,32,33,34] that the addition of a third component (%X) to the iron-carbon system will result in a change in the solubility of carbon (ΔC). According to these investigators the ratio ($\Delta C/\%X$) can be positive or negative and is independent of the temperature for most elements. Turkdogan et al. have indicated however a slight change in ($\Delta C/\%Mn$) as the temperature in increased.[35] With a standard state chosen so that $a_C = 1$ when the melt is saturated with carbon, a positive value of ($\Delta C/\%X$) for a given melt means the activity coefficient of carbon has decreased ($\gamma_C N_C = 1$).

The effect of magnesium upon carbon solubility in iron may be calculated from the experimental data for the Fe-C-Mg alloys previously discussed and the quantity ($\Delta C/\%Mg$) may be determined, Table II. The value is positive and decreases with increasing temperature. If the temperature effect is taken into account, the data can be represented by the equation:

$$\Delta C = K \times \%Mg \quad \text{where} \quad K = +0.129 \text{ at } 2300°F$$
$$K = +0.120 \text{ at } 2450°F$$
$$K = +0.106 \text{ at } 2600°F$$

Finally the effect of silicon may be superimposed. The factor ($\Delta C/\%Si$) has been determined for the simple Fe-C-Si system as -0.30 at 2900°F,[34] and for the data presented here is assumed to be independent of the temperature. It is now possible to calculate the combined effect of magnesium and silicon upon the solubility of carbon

TABLE II

EFFECT OF MAGNESIUM ON GRAPHITE SOLUBILITY

Heat No.	Temperature (°F)	Wt %Mg	Graphite Solubility (wt %) Fe-C System +	Fe-C-Mg System	ΔC/%Mg
CMT-68	2300	1.71	4.56	4.78	+0.129
CMT-80	2450	2.25	4.80	5.07	+0.120
CMT-73	2600	3.03	5.03	5.35	+0.106

+ Obtained from equation after Turkdogan and Leake[31] in the absence of a third component: $\log N_C = \frac{-560}{T} - 0.375$ where T is in °K.

TABLE III

JOINT EFFECTS OF MAGNESIUM AND SILICON ON GRAPHITE SOLUBILITY

Heat No.	Temperature(°F)	Chemical Analyses Wt%C	Wt%Si	Wt%Mg	Graphite Solubility in Fe-C System #	Changes in Graphite Solubility ΔC predicted +	ΔC actual °
CSMT-75	2300	4.65	0.50	1.76	4.56	+0.08	+0.09
CSMT-76	2300	3.87	2.87	1.50	4.56	-0.67	-0.69
CSMT-78	2600	4.40	2.82	2.56	5.03	-0.58	-0.63
CSMT-81	2600	5.07	0.68	2.80	5.03	+0.08	+0.04

As in Table II $\log N_C = \frac{-560}{T} - 0.375$

+ Predicted from equation $\Delta C = +Kx\%Mg - 0.30\ x\%Si$

where $K = +0.129$ at 2300°F

$K = +0.106$ at 2600°F

° Actual graphite solubility in Fe-C-Mg-Si system minus graphite solubility in Fe-C system.

and compare the calculations with the experimental data of Figure 17, Table III. In the calculations the joint effect is assumed to be the algebraic sum of the individual effects.

$$\Delta C = K \times \%Mg - 0.30 \times \%Si$$

where K is defined as previously for the Fe-C-Mg system.

The data in Table III indicate this basis for calculation is quite good. However, the difference between predicted and calculated solubility (0.01 to 0.05% C) becomes more apparent as the temperature is increased. The equation merely adds the independent effects of magnesium and silicon on graphite solubility and neglects the joint effects. It should be pointed out that higher silicon contents and higher temperatures may require the inclusion of higher order terms where the complex interaction of magnesium and silicon would also be taken into account.

3. Observations of Phases in Solid Samples

Although the emphasis in this research has been placed upon liquid-liquid equilibrium, some important information can be obtained by a study of the solid samples. The form of the carbon in the magnesium rich phase and of magnesium in the iron base phase are of particular interest. Metallographic examination, microhardness tests, and x-ray diffraction were employed to investigate the solid samples using rather conventional techniques.

The metallographic preparation is complicated by the fact that when an iron rich and a magnesium rich phase are present in the same

sample, they are extremely different in hardness and resistance to chemical action. For these reasons samples have to be polished in the complete absence of water with diamond used as the polishing agent rather than with the usual synthetic alumina, or magnesia suspensions. Since the diamond paste (1 micron) is not as fine as these suspensions, some scratches remain in the soft magnesium rich phase.

a. Structure of Iron Rich Layer (Heat No. CMT-73)

A micrograph of an unetched high carbon, 3% Mg-iron alloy is shown in Figure 20 indicating the presence of at least two phases. Examination of a spherical particle at higher magnification, Figure 21, shows it to be rather soft and containing what will be called a "sub-precipitate". The average microhardness values of these spherical particles is 46.1 kg/mm^2 with a 10.5 gm load. The matrix around the spherical particles on the other hand has a microhardness of 1095 kg/mm^2 with a load of 31 gms. (At microhardness levels less than 100 kg/mm^2, the hardness number is the same as that on the Vickers scale. However at 31 gm loads and a microhardness of 1100 kg/mm^2, the comparable Vickers hardness is approximately 1010 kg/mm^2.)

An x-ray diffraction pattern of the sample shows only the normal body centered cubic lines of ferrite and the orthorhombic lines of iron carbide. When the pattern is compared to one from an iron alloy of approximately the same carbon content and history except that it was not exposed to magnesium, the two patterns are found to be identical within the limits of experimental error. Since magnesium is sufficiently different in atomic size when compared to iron, approximately 20%, the

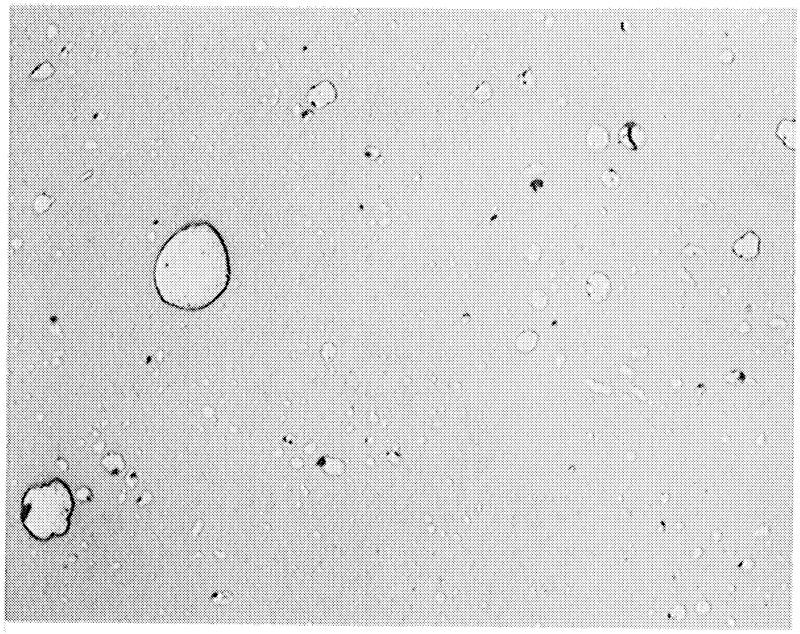

Figure 20. Photomicrograph of Iron Base Melt Unetched-100x - Heat No. CMT-73. Spherical Particles are Magnesium.

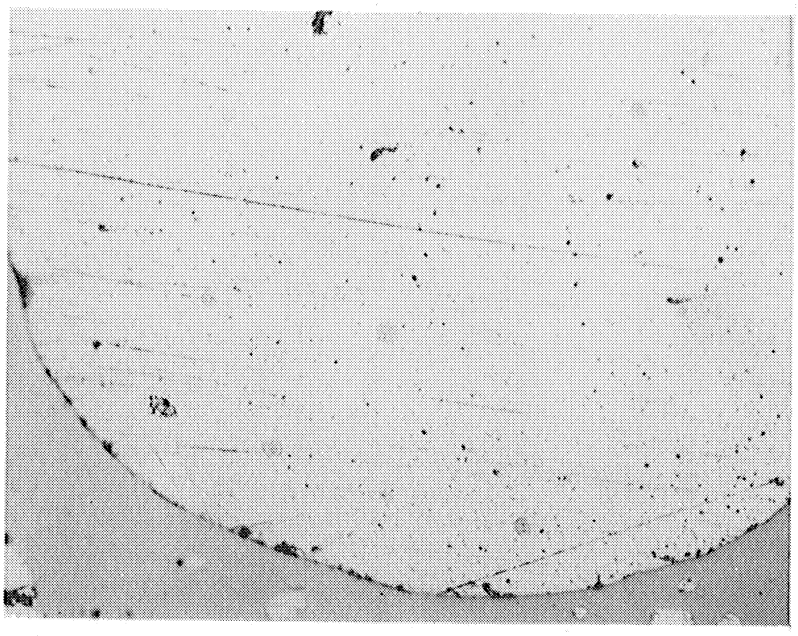

Figure 21. Photomicrograph of Iron Base Melt Unetched-500x - Heat No. CMT-73. Note Fine Precipitate in Magnesium Particle.

identical lattice parameter suggests that magnesium has very limited if any solid solubility in either ferrite or iron carbide. The lines from the magnesium rich phase were not expected in the x-ray diffraction pattern because of the small quantity.

The microhardness of pure magnesium (42.5 kg/mm^2 at 10.5 gm load) compares very favorably with that of the spherical precipitate in Figures 20 and 21. The slightly higher value for the precipitate could result from support by the iron carbide surrounding it and from the sub-precipitate. The same sub-precipitate is also found in the matrix of the magnesium base sample, Figure 22, where the matrix microhardness is 46.5 kg/mm^2 at a 10.5 gm load. It is therefore believed that the gross precipitate is very high in magnesium and of the same nature as the magnesium matrix in the magnesium base material.

b. Structure of Magnesium Rich Layer (Heat Nos. CM-63 and CMT-73)

As mentioned previously it is difficult to obtain representative samples of the magnesium liquid for an iron analysis due to the problem of settling of an iron rich constituent. This also leads to a problem in carbon analysis since it is believed that the carbon and iron would be closely associated. Figures 22 and 23 show a second phase within the magnesium matrix. In one case there is also shrinkage present, as might be expected when settling has taken place, while in the second case the presence of graphite flakes is also noted. Since the graphite is present only in the carbon saturated melts its existence is probably due to the mechanical entrapment of graphite from the eroded

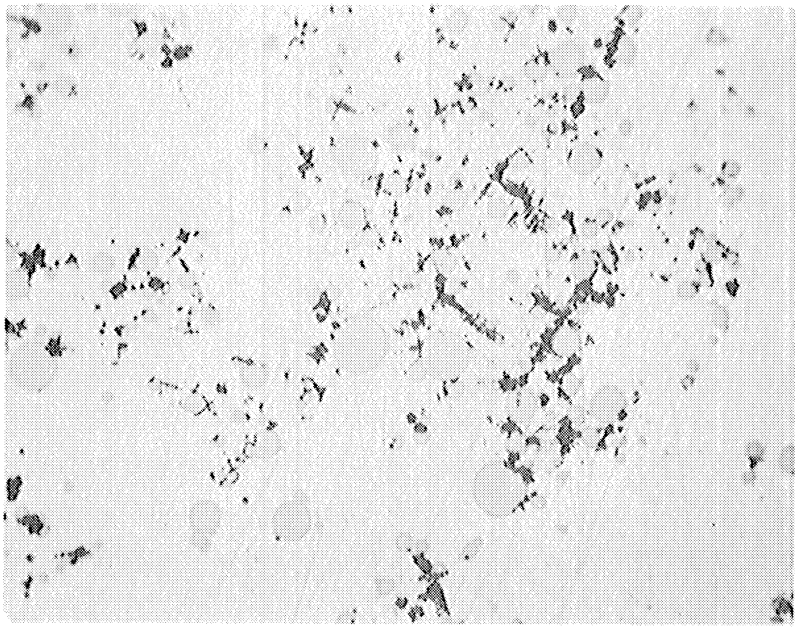

Figure 22. Photomicrograph of Magnesium Base Melt Unetched-100x - Heat No. CM-63. Note Presence of Shrinkage Associated with Spherical Iron Rich Phase.

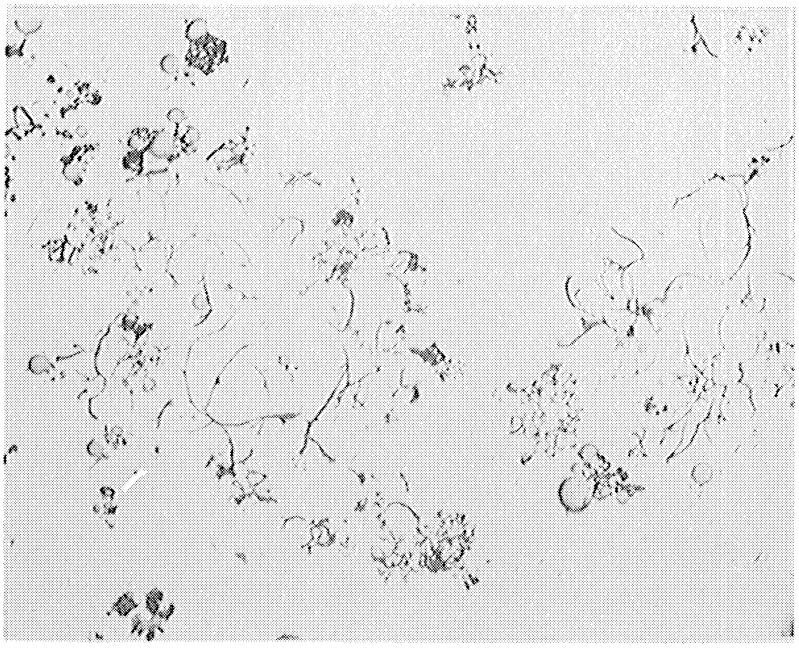

Figure 23. Photomicrograph of Magnesium Rich Phase Unetched-100x - Heat No. CMT-73. Note Presence of Graphite Flakes and an Iron Rich Phase.

crucible. For the carbon saturated melts, the problem of carbon analysis is therefore compounded.

An x-ray diffraction pattern of these samples indicates the presence of pure magnesium (no apparent change in lattice parameter) and iron carbide. The existence of relatively pure magnesium is not surprising as several investigators have indicated a very low solid solubility of iron in magnesium.(16,17,18,19,20)

A microhardness survey shows these iron rich particles in the magnesium have a microhardness of 1023 kg/mm^2 with a 31 gm load. This value compares very well with the value obtained for the iron carbide matrix in the iron base sample. The slightly lower figure could be attributed to poor support by the matrix. As a means of comparison in order that the microhardness values obtained would be more meaningful a survey has been carried out on vacuum melted iron with low impurities. The value is 144 kg/mm^2 at a 10.5 gm load for the relatively pure ferrite, practically an order of magnitude softer.

On the basis of x-ray diffraction and microhardnesses the secondary phase in the magnesium matrix therefore appears to be iron carbide. Also the sub-precipitate present in the magnesium particle of Figure 21 is thought to be iron carbide.

In general, the occurence of solid phases as occluded pools (iron carbide in magnesium and magnesium in iron carbide) suggests the possibility of a monotectic reaction. The monotectic temperature and composition are however unknown.

4. Engineering Applications of Solubility Relations

The greatest difficulty encountered in magnesium treatment of cast irons is the extreme vapor pressure of the magnesium which results in the general opinion of low magnesium solubility. The same conclusion can be reached even under an argon pressure blanket. As an example a melt of an Fe-C alloy was treated at 2500°F under pressure with excess magnesium outside the heating chamber but in the pressure vessel. After 20 seconds contact time between the two liquids, the samples were taken. This resulted in 0.04 Mg in an Fe-C alloy in which the saturated magnesium value is 1.40 Mg.

Non-equilibrium experiments have also lead to other opinions, such as the data of Zwicker[24] where the magnesium solubility is indicated to be lower than in the present investigation. Landa[25] has concluded that magnesium is in solid solution as shown by microhardness studies, however, the solid samples tested in the present research do not indicate solid solubility in either ferrite or carbide.

The establishment of the solubility data of course suggests several engineering applications relative to the production of nodular cast iron. The greatest potential is in the production of overtreated iron which could be diluted with untreated material. Two interesting experiments with high magnesium irons have been carried out which reflect the engineering potential of this procedure.

An Fe-C-Mg alloy was remelted under an argon blanket at atmospheric pressure. Chemical samples were taken at several time intervals after melt down. The initial magnesium content was 2.3% while the melt at melt down

contained 0.22%. The great loss of magnesium upon remelting was probably due to vapor loss upon heating.

Although remelting results in low magnesium recoveries, Figure 24 is an example of higher recoveries when an Fe-C-Mg alloy is used as an inoculant. The original melt to be inoculated contained only iron and carbon, whereas the Fe-C-Mg alloy contained 2 wt. pct. Mg. Although the recovery of the magnesium is high the amount of master alloy to be added is also high (50 gms Fe-C-Mg to 150 gms of Fe-C melt). However approximately 15 gms of Fe-C-Mg alloy could have been added with sufficient residual Mg for good nodule formation. The heavy master alloy without foreign elements such as Cu, Si, Ni, etc. offers definite advantages. It should also be pointed out that the reactivity of the addition is much less than that encountered with other master alloys of higher magnesium.

B. Thermodynamic Analysis of Interaction Among Elements Affecting Solubility

Although the principal purpose of this investigation was to ascertain the solubility of magnesium in iron-carbon and iron-carbon-silicon alloys, several conclusions can be reached concerning the activity and activity coefficients of the components. These results can be derived because of the necessary compatability of activity and phase equilibria, and are useful in explaining the solubility data. The presentation is concerned with: (1) definitions of interaction parameters, (2) calculation of interaction parameters in the Fe-C-Mg system, and (3) predicted parameters and observed experimental deviations.

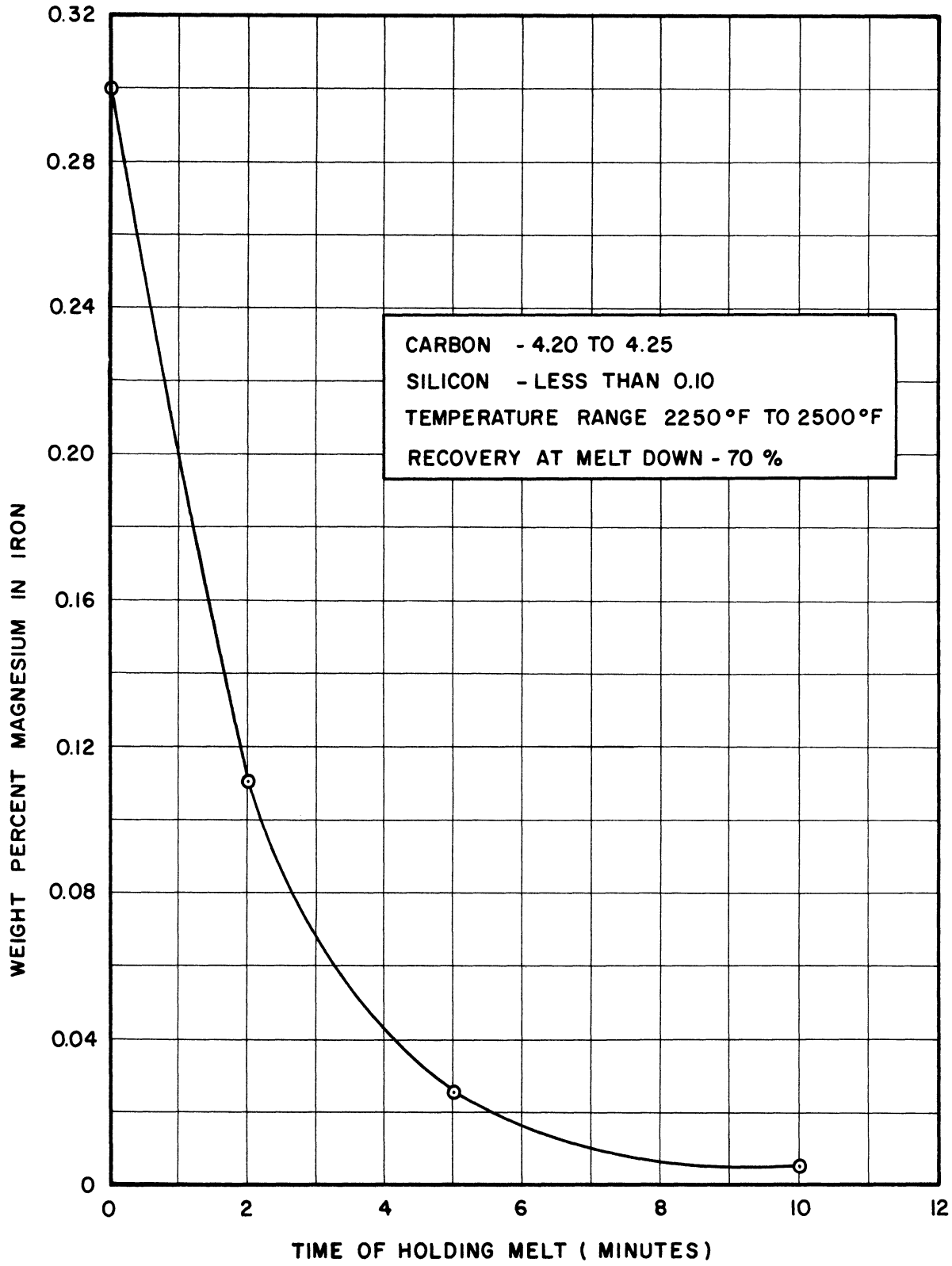

Figure 24. Rate of Loss of Magnesium from an Overtreated Cast Iron Melted Under an Argon Blanket. Treatment with high magnesium Fe-C-Mg alloy.

1. Definitions of Interaction Parameters

It has been pointed out in a previous section that the addition of a third component (X) to the iron-carbon system results in a change in carbon solubility ($\Delta C/\%X$). Several investigators have also suggested that the ratio ($\Delta C/\%X$) is a linear function of the atomic number of the added element X within a given period. In other words, elements in period III lie along one curve while elements in period IV lie along another curve, etc.[33,34]

The data for ($\Delta C/\%X$) can also be represented as an interaction parameter as derived from the definition of activity, a_C, and activity coefficient γ_C, for carbon as affected by small amounts of added element X:

$$\gamma_C N_C = a_C \qquad N_C = \text{mole fraction carbon}$$

or

$$\ln \gamma_C + \ln N_C = \ln a_C$$

since

$a_C = 1$ by definition, at carbon saturation

$\ln a_C = 0$ and $\ln \gamma_C = -\ln N_C$

If this relationship is differentiated with respect to N_X (the molar concentration of X) at constant activity of carbon, the following interaction parameter results:

$$\left(\frac{\partial \ln \gamma_C}{\partial N_X}\right)_{a_C} = -\left(\frac{\partial \ln N_C}{\partial N_X}\right)_{a_C} = \lambda_C^X$$

In the notation of Ohtani and Gokcen,[34] either one of these derivatives can be represented as the interaction parameter λ_C^X. Graphically

λ_C^X is most readily obtained from the negative slope of a plot of $\ln N_C$ versus N_X. Since $(\Delta C/\%X)$ is a function of the atomic number, the interaction parameter λ_C^X is also dependent upon the atomic number.

It is interesting to note that the activity of carbon can be held constant and at a different level by means other than carbon saturation. Fuwa and Chipman[33] accomplished this by the reaction: $CO_2 + \underline{C} = CO$, where the activity of carbon is held constant and is predetermined by the gas using a constant CO to CO_2 ratio. The addition of a third component will change the amount of carbon present in the melt, but the activity will be the same since the gas is the same. This gives rise to another interaction parameter. The major difference in the two interaction parameters is that one is evaluated under conditions of carbon saturation while the other is for solutions more dilute in carbon. The two interaction parameters can be close to one another, but they are in general not equal.

Wagner[36] has shown that interaction parameters are a consequence of the Gibbs-free energy equation and are generally <u>only</u> applicable in ternary systems at low concentrations of two of the elements. He therefore introduces the term ϵ defined in the Fe-C-X system as:

$$\epsilon_X^C = \left(\frac{\partial \ln \gamma_X}{\partial N_C}\right) \quad \text{and} \quad \epsilon_C^X = \left(\frac{\partial \ln \gamma_C}{\partial N_X}\right)$$

where

$$\epsilon_X^C = \epsilon_C^X \quad \text{only when} \quad N_C \rightarrow 0 \quad \text{and} \quad N_X \rightarrow 0$$

It should therefore be pointed out that ϵ_C^X and λ_C^X are derived for different conditions.

It is advantageous to define a new set of interaction parameters which are more general in nature, i.e., are not restricted to low amounts

of elements C and X or to evaluation at constant carbon activity. Ohtani and Gokcen[34] have accomplished this through an extension of the Wagner relationships and by evaluation of the Gibbs-Duhem equation for ternary systems. In their notation (with modification to the Fe-C-X system):

$$\zeta_C^X = \left(\frac{\partial \ln \gamma_C}{\partial N_X}\right)_{\frac{N_C}{N_{Fe}}} \quad \text{and} \quad \zeta_X^C = \left(\frac{\partial \ln \gamma_X}{\partial N_C}\right)_{\frac{N_X}{N_{Fe}}}$$

also

$$\zeta_C^X = \frac{N_{Fe} + N_X}{N_{Fe} + N_C} \zeta_X^C$$

If now the reference is to solutions close to carbon saturation (not constant a_C however) and to low concentrations of added element X, the following relationships can be derived:

$$\zeta_C^X = \left(\frac{\partial \ln \gamma_C}{\partial N_X}\right)_{\frac{N_C}{N_{Fe}}} \quad \text{and} \quad \zeta_X^C = \left(\frac{\partial \ln \gamma_X}{\partial N_C}\right)_{\frac{N_X}{N_{Fe}} \to 0} .$$

where

$$\zeta_C^X = N_{Fe}\, \zeta_X^C$$

In general the evaluation of ζ_C^X is most readily made by a knowledge of the change in γ_X as a function of N_C to obtain ζ_X^C, from which the last equation provides ζ_C^X.

2. Calculation of Interaction Parameters in Fe-C-Mg System

The interaction parameters of interest to this investigation are λ_C^{Mg} and ζ_C^{Mg}. However, before proceeding with the discussion of these parameters the activity coefficient of magnesium must be calculated from the data.

a. Activity Coefficient of Magnesium in the Fe-C-Mg System

It will be recalled in the application of Raoult's Law that a positive deviation indicates a greater tendency for like atoms to group together, whereas a negative deviation shows a greater attraction between solute and solvent atoms. Since there is an immiscibility gap in the magnesium-iron-carbon system, it is to be expected that a strong positive departure from Raoult's Law would be present.[37] Also since equilibrium is established between the two liquid layers, the chemical potential of a given component in each liquid must be the same. With a standard state of pure magnesium ($a_{Mg} \rightarrow 1$ when $N_{Mg} \rightarrow 1$), the activity coefficient of magnesium in the iron base liquid can be calculated if Raoult's Law is assumed for the magnesium base liquid.

The justification for the use of Raoult's Law is apparent from the summary of the magnesium activity coefficients in Table IV. $N_{Mg}^{(1)}$ is greater than 0.98 and the predicted positive deviation would result in very little change in the calculated value of $\gamma_{Mg}^{(2)}$. It will be noted however that carbon has been neglected in the calculation of $N_{Mg}^{(1)}$. As pointed out in a previous section, carbon appears to be present as iron carbide in the solid samples. Therefore a short calculation would indicate that the maximum effect of carbon on $N_{Mg}^{(1)}$ would be to lower this value by approximately 0.004, if the ratio of 3:1 is maintained between iron and carbon (Fe_3C). In the absence of actual carbon analyses, the mole fraction carbon has been assumed to be zero in the magnesium due to its very small effect.

Figure 25 is a plot of the activity coefficient of magnesium versus the mole fraction carbon in the iron base melt, which is developed from solubility plots in Figures 16 and 18.

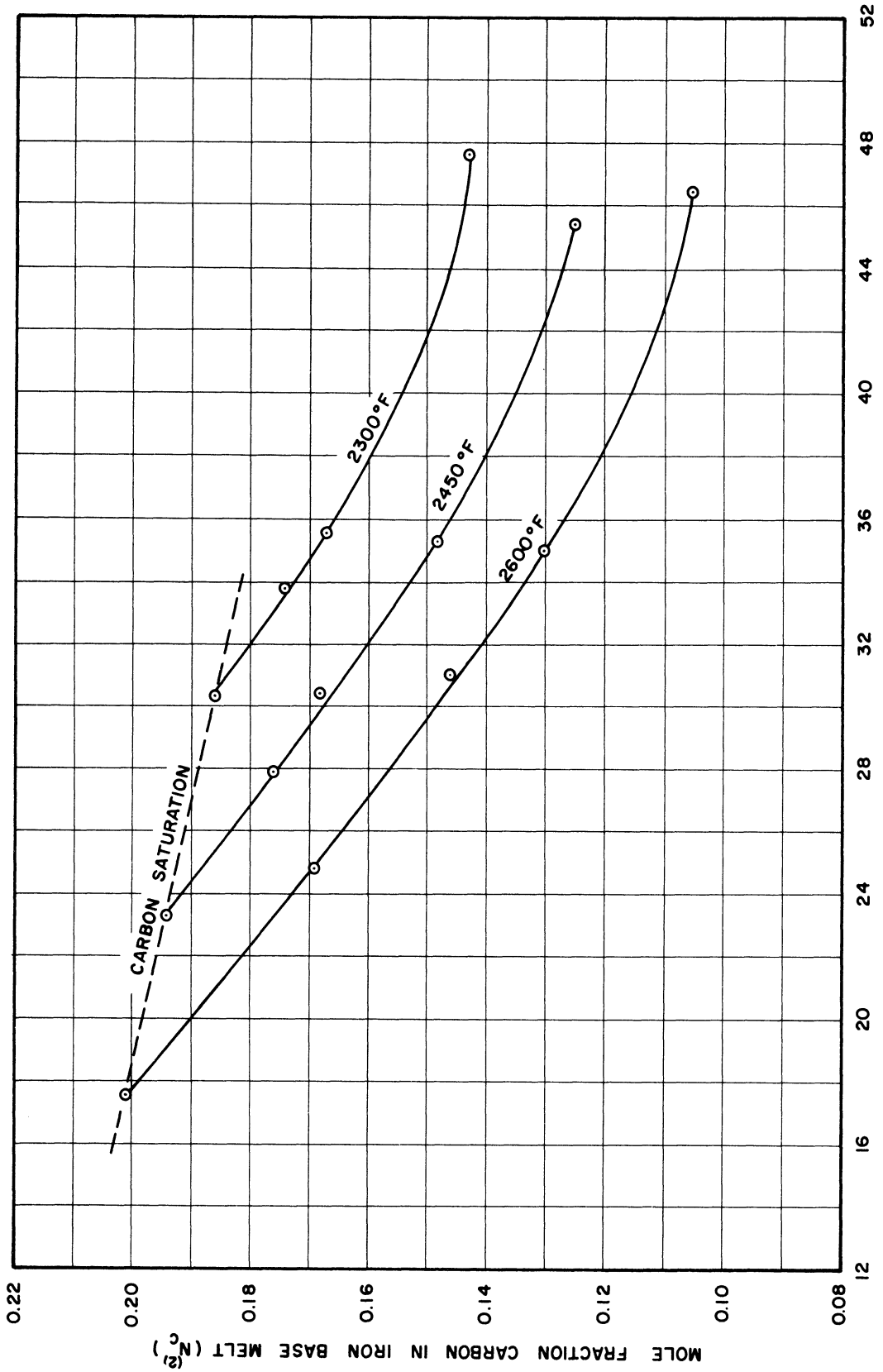

Figure 25. Activity Coefficient of Magnesium in the Iron Base Liquid as Affected by the Carbon Content.

TABLE IV

ACTIVITY COEFFICIENTS OF MAGNESIUM IN IRON BASE MELT

Heat No.	Temperature (°F)	Magnesium Base Melt (Liquid 1) # $N_{Fe}^{(1)}$	$N_{Mg}^{(1)}$	Iron Base Melt (Liquid 2) $N_{Mg}^{(2)}$	$N_{Fe}^{(2)}$	$N_{C}^{(2)}$	$\gamma_{Mg}^{(2)}$ *
CM-52+	2450	.00792	.9921	.0355	.788	.176	27.9
CM-57+	2450	.00655	.9935	.0219	.853	.125	45.4
CM-58	2600	.01025	.9898	.0319	.822	.146	31.0
CM-60	2300	.00628	.9937	.0294	.796	.174	33.8
CM-61	2600	.01096	.9890	.0398	.791	.169	24.8
CM-63	2600	.00908	.9909	.0283	.841	.130	35.0
CM-64	2600	.00828	.9917	.0214	.873	.105	46.3
CM-66	2300	.00571	.9943	.0209	.835	.143	47.6
CM-67	2450	.00712	.9929	.0281	.823	.148	35.3
CMT-68	2300	.00641	.9936	.0328	.781	.186	30.3
CMT-73+	2600	.01294	.9871	.0563	.742	.201	17.5
CM-74	2450	.00792	.9921	.0326	.799	.168	30.4
CM-79+	2300	.00615	.9939	.0280	.804	.167	35.5
CMT-80	2450	.00882	.9912	.0425	.763	.194	23.3

Based upon zero carbon present

* Standard State $a_{Mg}^{(2)} = a_{Mg}^{(1)} \longrightarrow 1$ when $N_{Mg}^{(1)} \longrightarrow 1$ (pressures greater than vapor pressure of pure magnesium)

$$\gamma_{Mg}^{(2)} = \frac{a_{Mg}^{(2)}}{N_{Mg}^{(2)}} = \frac{a_{Mg}^{(1)}}{N_{Mg}^{(2)}} = \frac{N_{Mg}^{(1)}}{N_{Mg}^{(2)}}$$

+ Data partially obtained from solubility curves.

TABLE V

INTERACTION PARAMETERS IN Fe-C-Mg SYSTEM

Temperature (°F)	$(N_{Fe})_{N_{Mg} \longrightarrow 0}$	ζ_{Mg}^{C} *	ζ_{C}^{Mg} +
2300	0.818	-10.25	-8.30
2450	0.810	-10.00	-8.10
2600	0.803	-10.11	-8.10

* $\zeta_{Mg}^{C} = \left(\frac{\partial \ln \gamma_{Mg}}{\partial N_C}\right)_{\frac{N_{Mg}}{N_{Fe}}}$ from 0.02 to 0.07

(Obtained from slope of curves in Figure 27)

+ $\zeta_{C}^{Mg} = (N_{Fe})_{N_{Mg} \longrightarrow 0} \times \zeta_{Mg}^{C}$

b. Interaction Parameters λ_C^{Mg} and ζ_C^{Mg}

It will be recalled that λ_C^{Mg} is generally evaluated by varying the mole fraction of magnesium at constant temperature and determining the carbon solubility. In the present investigation only one such point has been obtained at each temperature where the melt is doubly saturated (with carbon and magnesium). However, it is also known that N_C at $N_{Mg} = 0$ must be governed by the equation: $\log_{10} N_C = \frac{-560}{T} - 0.375$.[31] With this knowledge a plot of $\ln N_C$ at carbon saturation versus N_{Mg} is included in Figure 26. The following values are obtained for

$$\lambda_C^{Mg} = -\left(\frac{\partial \ln N_C}{\partial N_X}\right)_{a_C = 1}$$

Temperature	λ_C^{Mg}
2300°F	-0.68
2450°F	-0.54
2600°F	-0.30

It is again apparent that λ_C^{Mg} is temperature dependent, which is to be expected since $(\Delta C/\%Mg)$ shows a temperature dependency.

The carbon interaction parameter at concentrations other than those which result in unit carbon activity is given as ζ_C^{Mg} where:

$$\zeta_C^{Mg} = N_{Fe}\, \zeta_{Mg}^{C} \ (\text{at} \ \ N_{Mg} \to 0) = N_{Fe} \left(\frac{\partial \ln \gamma_{Mg}}{\partial N_C}\right)_{\frac{N_{Mg}}{N_{Fe}} \to 0}$$

Figure 27 is a plot of $\ln \gamma_{Mg}$ versus N_C where the ratio (N_{Mg}/N_{Fe}) varies between 0.02 and 0.07. Since the three isotherms are essentially straight lines, the parameter ζ_{Mg}^{C} is the slope of the lines. Table V is a summary of values for ζ_{Mg}^{C} and ζ_C^{Mg}. Again there is only some slight temperature dependency. For this reason the value of ζ_C^{Mg} might be taken to be approximately -8.1 from 2300 to 2600°F.

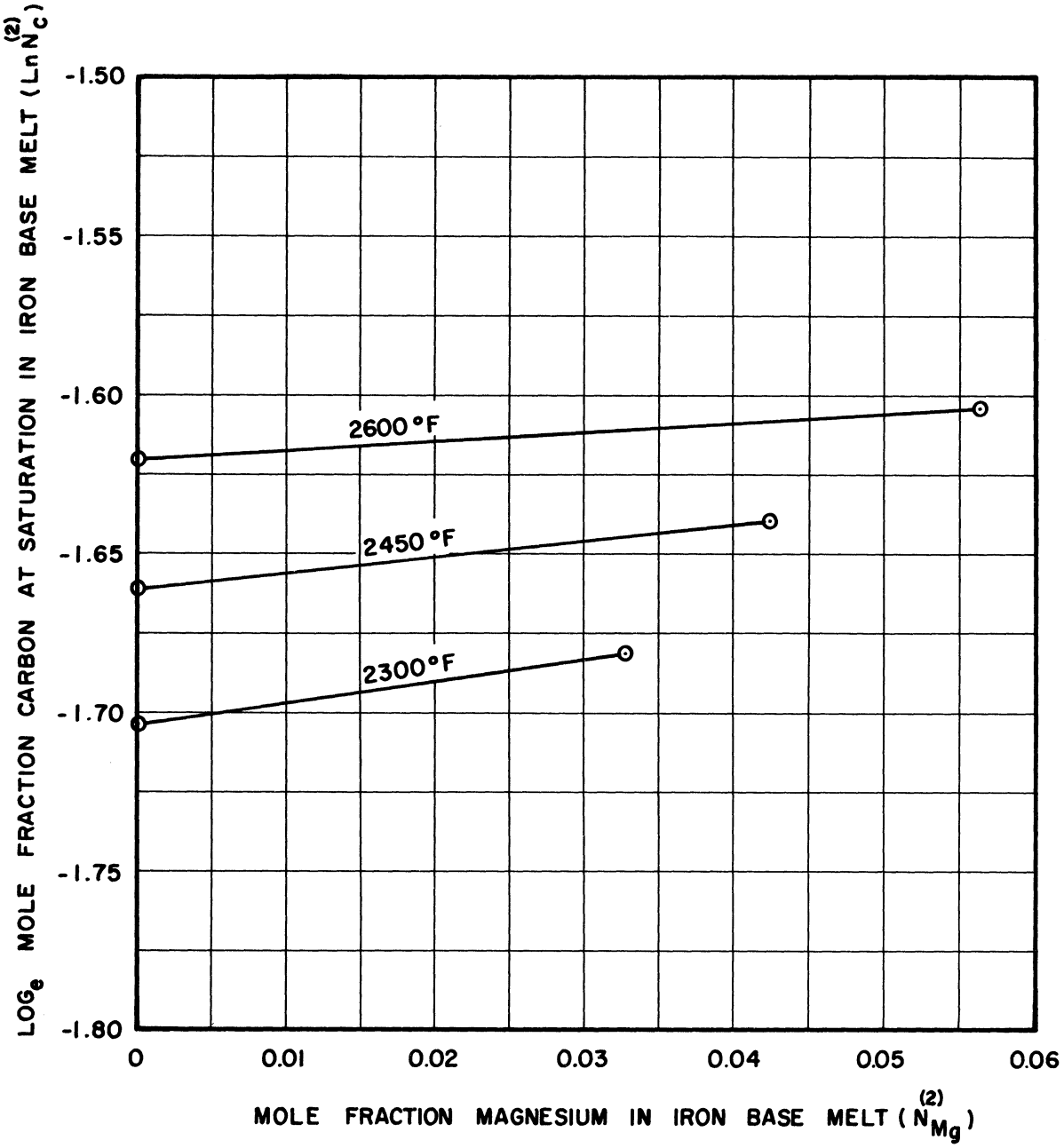

Figure 26. Effect of Magnesium Upon the Carbon Solubility in Iron Base Liquid.

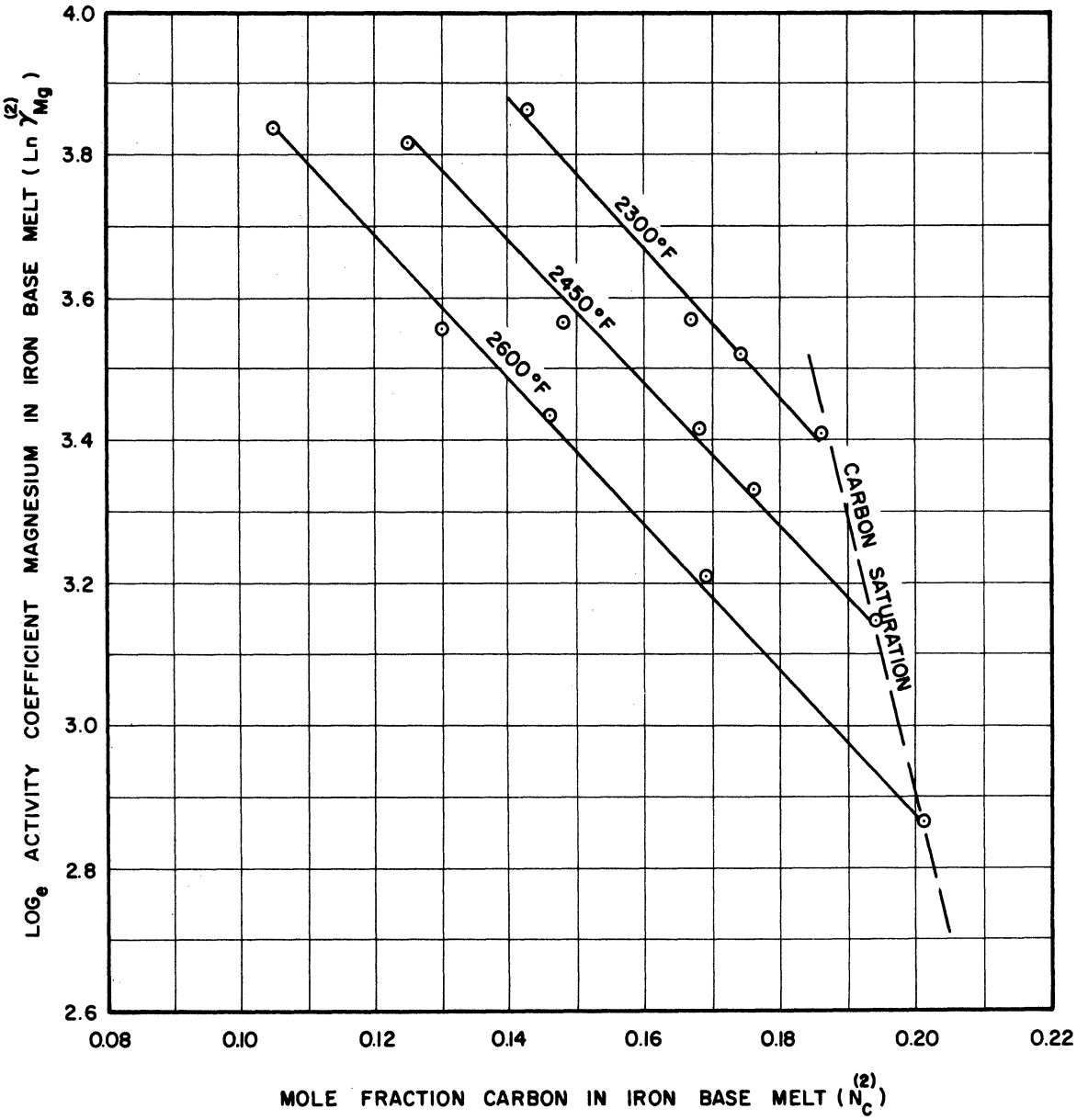

Figure 27. Logarithmic Variation in the Activity Coefficient of Magnesium as Affected by Carbon Content in the Iron Base Liquid.

3. Predicted Parameters and Observed Experimental Deviations

The interaction parameters and carbon solubility data are interesting in the light of recent predictions for these values. Due to the indication of a periodic relationship among the elements, Ohtani and Gokcen extrapolated their data to include elements where solubility data were missing.[34] Below is a summary of their predictions for magnesium and the current experimental data:

	Temperature (°F)	(ΔC/%Mg)	λ_C^{Mg}	ζ_C^{Mg}
(Experimental)	2300	+0.129	-0.68	-8.30
(Experimental)	2450	+0.120	-0.54	-8.10
(Experimental)	2600	+0.106	-0.30	-8.10
(Predicted)	2900	-0.20	+2.0	+3.30

Although the predicted values are for higher temperatures, it can be readily seen that they are incompatible with the experimental results. An increase in 300°F from the 2600°F data would not be expected to bring the values to an equivalent magnitude. However the experimental results can be explained with the aid of a thermodynamic development by Alcock and Richardson.[38]

In general the extension of the Alcock and Richardson equations for the Fe-C-X system would be as follows for dilute solutions in element X:

$$\epsilon_C^X = \left(\frac{\partial \ln \gamma_C}{\partial N_X}\right)_{N_X \to 0} = \ln \gamma_{C(X)} - \ln \gamma_{C(Fe)} - \ln \gamma_{X(Fe)}$$

where

$\gamma_{C(X)}$ = activity coefficient of carbon in element X

$\gamma_{C(Fe)}$ = activity coefficient of carbon in iron

$\gamma_{X(Fe)}$ = activity coefficient of element X in iron

In addition to assuming dilute solutions, this equation is based upon equal coordination numbers for the three atom species and random distribution of the atoms.

The interaction parameter in the ternary system is therefore dependent upon the activity coefficients in the three binaries. More important, since at a given temperature $\ln \gamma_{C(Fe)}$ is a constant (positive), the interaction parameter is basically a function of $\ln \gamma_{C(X)}$ and $\ln \gamma_{X(Fe)}$.

Consider the interaction parameter in the form below which is comparable to the parameter ζ_C^{Mg}:

$$\epsilon_C^{Mg} = \left(\frac{\partial \ln \gamma_C}{\partial N_{Mg}}\right)_{N_{Mg} \to 0} = \ln \gamma_{C(Mg)} - \ln \gamma_{C(Fe)} - \ln \gamma_{Mg(Fe)}$$

A large negative value for ϵ_C^{Mg} will be obtained if $\ln \gamma_{C(Mg)}$ is negative and(or) if $\ln \gamma_{Mg(Fe)}$ is strongly positive. Magnesium is known to form several carbides, however the recognized carbides are thought to decompose at relatively low temperatures. It is interesting to recall that magnesium carbide did not exist in the quenched samples at room temperature. However this does not preclude the possibility of a magnesium carbide in a slowly cooled specimen or a free energy inversion between magnesium carbide and iron carbide as the temperature is lowered.

It therefore appears that $\ln \gamma_{C(Mg)}$ is not strongly negative, if at all. However the possibility of a large positive value for

$\ln \gamma_{Mg(Fe)}$ is pointed out by the data. Although the exact value of the activity coefficient of magnesium is unknown $(N_C \rightarrow 0)$, Figures 25 and 27 indicate the value to be very large. Therefore $\ln \gamma_{Mg(Fe)}$ is strongly positive which could account for a negative value for ϵ_C^{Mg} (or ζ_C^{Mg}). It might also be pointed out that the possibility of clustering is excluded in the derivation of ϵ_C^{Mg}. However due to immiscibility in the Fe-C-Mg system the effect of short range order in the liquids could have a very pronounced effect on the value of the interaction parameter.

It is apparent in the general case that a negative interaction parameter, ζ_C^X, does not necessarily mean a strong carbide forming element is present, since a strong repulsion between iron and element X could also produce the same result. By a similar argument, a positive interaction parameter need not merely reflect a low carbon-element X attraction, but can also indicate a strong iron-element X bond as is the case with silicon.

The data of Ohtani and Gokcen also indicate a periodic relationship which forms the basis for their predictions for magnesium. It should be pointed out again that the periodic relationship has greater implications than merely a carbon-element X interaction. If several of the transition elements are considered, (titanium to copper) there is a gradual change from strong carbide forming tendency to non-formation of carbides as the atomic number is increased. The carbide forming tendency is periodic in nature as evidenced by the free energy of formation. However, in order for ϵ_C^X to be periodic, the value $\ln \gamma_{X(Fe)}$ must also change uniformly with the atomic number. It can be readily appreciated this requires a very dominant periodicity and it may be anticipated that several exceptions can occur.

Aluminum, silicon, phosphorus, and sulfur (considered as elements in the third period or series) all form compounds with iron with the net result of negative values for $\ln \gamma_{X(Fe)}$ or positive values for ϵ_C^X. Consider the difficulty presented when magnesium (Z = 12) is compared to aluminum (Z = 13). Aluminum derives its positive value, ϵ_C^{Al}, from a strong negative deviation from Raoult's Law in the Fe-Al system ($\ln \gamma_{Al(Fe)}$ is negative). Magnesium however has a strong positive deviation from Raoult's Law due to immiscibility which results in a large negative value for ϵ_C^{Mg}. It is therefore extremely difficult to link the two elements aluminum and magnesium together periodically.

It is however possible the periodic group effect becomes more predominant for the alkali and alkaline earth metals, as it is anticipated that liquid immiscibility occurs between these elements and iron. Therefore the values of $(\Delta C/\%X)$, λ_C^X, and ζ_C^X may result in a separate periodic relationship for Li, Na, K, etc. and for Be, Mg, Ca, etc.

It might be mentioned that the thermodynamics can be considered in terms of atom bonds which is essentially the technique of Alcock and Richardson in their derivation of ϵ_C^X. In the Fe-C-Si-Mg system the effect of atom bonds upon solubility is therefore apparent. If iron atoms prefer iron atoms and magnesium atoms prefer their own species as manifested in the liquid immiscibility, the problem reduces to one of finding other atoms which will reduce the iron-magnesium incompatability. Carbon and silicon appear to do this. In fact, it might be anticipated that other atoms would accomplish a similar effect in other binary systems with wide immiscibility gaps.

CONCLUSIONS

The investigations of solubility in the Fe-C-Mg and Fe-C-Mg-Si systems have indicated that an open system in which an inert gas is applied at a greater pressure than the vapor pressure of magnesium can be used to advantage to investigate liquid-liquid equilibrium. The same general technique can now be applied to other systems with equivalent characteristics. In general this investigation not only provides engineering data as manifested by the magnesium solubility, but also interrelates solubility with thermodynamic parameters.

In the temperature range explored (2300-2600°F) the carbon content is more important in determining the solubility of magnesium than the temperature itself. In general silicon also increases magnesium solubility, however due to the carbon dependency the net effect can be to decrease the maximum solubility since silicon lowers the solubility of carbon.

Magnesium increases the carbon solubility to a greater extent at low temperatures than at high temperatures. In general the combined effect of magnesium and silicon on graphite solubility can be represented by the equation: $\Delta C = Kx\%Mg - 0.30x\%Si$ where K is 0.129 at 2300°F and 0.106 at 2600°F.

Other investigators predict that magnesium should decrease the solubility of graphite and that the interaction parameters below should be positive in sense:

$$\lambda_C^{Mg} = -\left(\frac{\partial N_C}{\partial N_{Mg}}\right)_{a_C} \qquad \zeta_C^{Mg} = \left(\frac{\partial \ln \gamma_C}{\partial N_{Mg}}\right) \frac{N_C}{N_{Fe}}$$

Experimental values however obtained from carbon solubility studies and calculation of activity coefficients of magnesium in the iron base melt indicate these parameters are negative. The general explanation for these data does not necessarily depend upon a great affinity between magnesium and carbon atoms. Instead a very large repulsion between iron and magnesium atoms can be the dominating factor. It is therefore anticipated that a similar explanation and a non-adherence to published periodic effects may exist in other systems where liquid immiscibility may occur with Fe-C alloys.

APPENDIX

FURNACE CONSTRUCTION

The furnace used in this study is composed of three basic units: pressure shell; heating chamber; remote control and sampling mechanisms.

Pressure Shell (Figures 4, 10, 11)

The pressure shell is essentially in two parts: the shell with a bottom and flange welded to it, and a removable cover which bolts to the flange. The entire vessel with all exit ports has been designed according to the API-ASME Boiler Code for Unfired Pressure Vessels to withstand an internal pressure of 500 pounds per square inch gauge. All of the components have been made of Type 304 stainless steel. The internal working volume is approximately 14 inches in diameter, 26 inches deep.

An inner shell made of copper is also provided to which has been soldered water cooled coils of copper tubing. The inner shell first reduces heating of the main container by convection of the argon atmosphere and radiation from the melt. Also, and probably more important, the copper shell prevents eddy current losses in the stainless steel by turning the magnetic field inward. (This compact field design will even prevent heating of a bar of ferritic steel which is held four inches from the coil.)

Extensive use has been made of "O" ring seals for the components which must move; such as around the rods of the turning mechanism. These seals have also been used for the 1 inch thick window port in the cover and around the power leads to the coil. The power leads have to be insulated from the steel to prevent shorting, therefore they are supported by

a nylon insert which contains the "O" ring grooves. In order to avoid overheating of the shell at the power lead exit, the port is hollow and is water cooled.

The thermocouple ports are sealed against pressure leaks by using rubber and nylon plugs with fine holes. Upon tightening a retaining ring on the outside of the vessel, the rubber is compressed against the wire thereby effecting a fairly efficient seal.

Argon is introduced into the shell from a compressed gas bottle through flexible rubber pressure tubing. The gas connection to a main manifold is terminated in a valve to which is connected a vacuum pump for pre-evacuation. At all times the pressure or vacuum can be read from one of the three gauges on the control panel. The particular gauge in use is determined by the pressure to be used for a given run.

Before the shell was placed in service the unit was hydrostatically tested at 750 pounds per square inch gauge. Although the vessel showed no leaks, certain precautions have been taken for a higher degree of safety. As an example the viewing port is never used directly but rather an inclined mirror reduces the hazard of direct observation in the event the glass port should fail. Also a pressure release valve is attached to the shell. One of four valves with set pressures of 125, 250, 375, and 500 psig is selected; the choice is dependent upon the operating pressure. In the event of a pressure leak and a subsequent magnesium fire, a suitable fire extinguisher for such metal fires is available in close proximity to the pressure equipment.

It is seen that the equipment is mounted on wheels which makes it somewhat portable, although the total weight is approximately 600 pounds.

Heating Chamber (Figures 5, 6, 7, 11)

A thirteen turn copper coil of 1/4 inch OD tubing is wound on a fused silica form and covered with a chemical setting Sauereisen cement. The inside of the silica shell is coated with a mixture of a Sauereisen cement plus 10% TiO_2, then a piece of Al_2O_3 insulating brick is cemented to the inside. The radiant loss is therefore low which is evidenced by only 5 KW required to hold a melt at 2600°F.

The graphite susceptor is made in two pieces. Approximately one-half the power is induced into the susceptor while some power is still induced into the melt. The susceptor therefore provides a chamber of constant temperature. The crucible, lower section of the susceptor, refractory base, and transite base can be lowered out of the heating zone. The upper part of the susceptor, refractory cover, and thermocouple protection tube are therefore held stationary by an alumina hanger. The hanger is made by ramming Alundum cement into a pattern where after ejection it is fired at 2500°F. The crucible covers of alumina are made by the same technique, however, the covers and upper portions of the crucible have to be coated with a colloidal graphite solution to prevent adhesion between these two pieces during melting.

It might be mentioned that the heating chamber design does not allow for different power taps (power is across the full coil). For this reason difficulty has been encountered in matching the inductance of coil and charge. However, dummy windings have been used outside the shell which are essentially used in power dissipation. With this set up it is possible to operate at power settings up to 15 KW.

Remote Control and Sampling Mechanisms (Figure 8, 9, 10, 13)

Means have been devised to raise, lower, and turn the crucible from outside the pressure vessel. The crucible and its lower supports are raised and lowered by means of a rack and pinion arrangement. When the rod, to which the pinion gear is attached, is turned the nylon rack rides up or down in a brass retaining cylinder. The transite platform and crucible are carried up or down by the rack which is hollow and contains another stainless steel rod. This rod exits through the bottom of the pressure vessel. When the rack is at its lowest point the lower steel rod engages the nylon rod of the transite platform and the crucible can be rotated under the sampling device.

The sampling device consists of two tubes, one of steel to sample the magnesium and one of fused silica to sample the iron base melt. The two tubes are connected by means of glass and rubber tubing to an orifice inside the pressure vessel. Outside the vessel are two needle valves and a flowmeter which allow adjustment for changes in internal pressure. In general the first needle valve is opened enough to give a desired flowrate when the second valve is wide open. The necessary flowrate to provide sound samples is determined by trial and error. Of course higher flowrates are required for higher operating pressures. In order to prevent flow of molten metal outside the sample tubes, steel stops with three - 1/32" holes are placed at the top of the sample tubes. Although the liquid metal rises fairly fast initially, the outer needle valve is left open approximately 5 seconds and at this time the indicated flowrate has dropped to zero.

BIBLIOGRAPHY

1. White, R. W. "Magnesium Treatment Techniques." Journal of Metals, Vol. 12, June, 1960, p. 464-466.

2. Ihrig, H. K. "New Nodular Iron Process." Metals Progress, 70:154, September, 1956, U.S. Patent 2,750,284, June, 1956.

3. Paranjape, Vishnu K. India Patent 45,760, August, 1953.

4. Yoda, Rempei, "Iron Treated with Magnesium Nitride." Nippon Kinzoku Gakkai-Shi, Tokyo Inst. of Tech. 18, 250-5, 1954, U.S. Patent 2,757,086, July, 1956 (INCO).

5. Wittmoser, A. "The Ladle Treatment of Cast Iron with Metallic Magnesium." Giesserei, Vol. 41, No. 5, March, 1954, p. 105-108.

6. Mitsche, R. and Onitsch-Modl, E. M., Austrian Patents 177,794 and 177,795, March, 1954.

7. Langaretti, C. and Noris, M. "New Process for Nodular Iron Production at Low Treatment Cost." Trans. AFS, Vol. 60, 1952, p. 101-107.

8. Ziffer, L. P. Introduction of Magnesium into Liquid Iron, U.S. Patent 2,678,267, May, 1954.

9. The Treatment of Liquid Iron with Gaseous Metals, Swiss Patent 291,858, October, 1953.

10. Langaretti, C. "Italian Production of Nodular Cast Iron by Means of Metallic Magnesium." Giesserei, Vol. 41, No. 16, August, 1954, p. 410-412, Italian Patent 485,770, 1953.

11. Hlousek, C. and Hostinsky, Z. "Inoculation of Cast Iron with Magnesium in an Autoclave." Slevarenstvi, Vol. 2, No. 6, Prace Ceskoslovenskeho Vyzkumu Slevarenskeho, Vol. 1, No. 6, 1954.

12. Otahol, V. "Industrial Production of Spheroidal Cast Iron at High Pressure." Slevarenstvi, Vol. 3, No. 1, January, 1955, p. 2-6.

13. "Magnesium Addition in a Closed Vessel." Engineering, Vol. 180, July 15, 1955, p. 88.

14. Mond Nickel Co., British Patents 743,456 and 743,469, 1956.

15. Zwicker, V. U.S. Patent 2,754,201, July, 1956, Gradpierre, M.C.M., U.S. Patent 2,781,260, February, 1957 (INCO).

16. Fahrenhorst, E. and Bulian, W. Z. Metallkunde, Vol. 33, 1941, p. 31, Vol. 34, 1942, p. 166.

17. Beerwald, A. Metallwirtschaft, Vol. 23, 1944, p. 404.

18. Siebel, G. Z. Metallkunde, Vol. 39, 1948, p. 22.

19. Mitchell, D. W. Trans. AIME, Vol. 175, 1948, p. 570.

20. Yue, A. S. The Dow Metal Products Company, Midland, Michigan, (Private Communication).

21. Busk, R. S. Trans. AIME, Vol. 188, 1950, p. 1464.

22. Private Communication with the Dow Metal Products Company on the Mg-Si System.

23. Schneider, A. and Cordes, J. F. "Mg-C System." Zeitschrift fur Anorganische Chemi, Vol. 279, 1955, p. 94.

24. Zwicker, V. "Reactions Between Some Magnesium Alloys and Liquid Cast Iron." Z. Metallkunde, Vol. 45, 1954, p. 31.

25. Landa, A. F. "Solubility of Magnesium in Cast Iron." Liteinoe Proizvodstvo, No. 8, 1957, p. 27-29.

26. Selected Properties for the Thermodynamic Properties of Metals and Alloys, Mineral Research Laboratory, University of California, November, 1956.

27. Case, L. O. Elements of the Phase Rule, The Edwards Letter Shop, Ann Arbor, Mich., 1939.

28. Seybolt, A. U. and Burke, J. E. Procedures in Experimental Metallurgy, John Wiley and Sons, New York, 1953.

29. Schneider, V. A. and Stoll, E. K. Zeitschrift Fur Elektrochemie, Vol. 47, 1941, p. 519.

30. Chipman, J., Fulton, J. C., Gokcen, N. and Caskey, G. R. "Activity of Silicon in Liquid Fe-Si and Fe-C-Si Alloys." Acta Metallurgica, Vol. 2, No. 3, 1954, p. 439-451.

31. Turkdogan, E. T. and Leake, L. E. "Thermodynamics of C in Iron Alloys." Iron and Steel, November, 1955, p. 567-574.

32. Ohtani, M. "On Activities of Si and C in Molten Fe-Si-C Alloys." Sci. Rep. Res. Inst., Tohoku Univ., Vol. A7, 1955, p. 487-501.

33. Chipman, J., Fuwa, T. "Activity of Carbon in Liquid Iron Alloys." Trans. AIME, Vol. 215, 1959, p. 708-716.

34. Ohtani, M , and Gokcen, N. A. "Thermodynamic Interaction Parameters of Elements in Liquid Iron." Trans. AIME, Vol. 218, No. 3, 1960, p. 533-540.

35. Turkdogan, E. T., Hancock, R. A., Herlitz, S. I., and Dentan, J. Journal of Iron and Steel Inst., 1956, Vol. 183, p. 69.

36. Wagner, C. Thermodynamics of Alloys, Addison Wesley Press, 1952, p. 51.

37. Darken, L. S. and Gurry, R. W. Physical Chemistry of Metals, McGraw-Hill Book Company, 1953.

38. Alcock, C. B. and Richardson, F. D. "Dilute Solutions in Molten Metals and Alloys." Acta Metallurgica, Vol. 6, June, 1958, p. 385-395.